



**Nebraska  
Transportation  
Center**



**MID-AMERICA  
TRANSPORTATION CENTER**

**NEBRASKA**

Good Life. Great Journey.

**DEPARTMENT OF TRANSPORTATION**

**Report SPR-P1 (17) M055**

**Final Report**  
26-1121-4034-001

## **New Mixture Additives for Sustainable Bituminous Pavements**

### **Gabriel Mukristu Nsengiyumva**

Graduate Research Assistant  
Department of Civil Engineering  
University of Nebraska-Lincoln

### **Santosh Reddy Kommidi**

Graduate Research Assistant

### **Yong-Rak Kim, Ph.D.**

Professor

### **Helan Xu, Ph.D.**

Post-Doctoral Fellow

### **Yiqi Yang, Ph.D.**

Professor

---

2018

Nebraska Transportation Center  
262 Prem S. Paul Research Center at Whittier School  
2200 Vine Street  
Lincoln, NE 68583-0851  
(402) 472-0141

"This report was funded in part through grant[s] from the Federal Highway Administration [and Federal Transit Administration], U.S. Department of Transportation. The views and opinions of the authors [or agency] expressed herein do not necessarily state or reflect those of the U.S. Department of Transportation."

## **New Mixture Additives for Sustainable Bituminous Pavements**

Gabriel Mukristu Nsengiyumva  
Graduate Research Assistant  
Department of Civil Engineering  
University of Nebraska-Lincoln

Santosh Reddy Kommidi  
Graduate Research Assistant  
Department of Civil Engineering  
University of Nebraska-Lincoln

Yong-Rak Kim, Ph.D.  
Professor  
Department of Civil Engineering  
University of Nebraska-Lincoln

Helan Xu, Ph.D.  
Post-Doctoral Fellow  
Textiles, Merchandising & Fashion Design  
University of Nebraska-Lincoln

Yiqi Yang, Ph.D.  
Professor  
Textiles, Merchandising & Fashion Design  
University of Nebraska-Lincoln

A Report on Research Sponsored by

Nebraska Department of Transportation

May 2018

## Technical Report Documentation Page

1. Report No SPR-P1(17) M055	2. Government Accession No.	3. Recipient's Catalog No.	
4. Title and Subtitle  New Mixture Additives for Sustainable Bituminous Pavements		5. Report Date May, 2018	
		6. Performing Organization Code	
7. Author/s Gabriel Mukristu Nsengiyumva, Santosh Reddy Kommidi, Yong-Rak Kim, Helan Xu and Yiqi Yang		8. Performing Organization Report No.	
9. Performing Organization Name and Address Nebraska Transportation Center University of Nebraska-Lincoln (Department of Civil Engineering) 362N WHIT, 2200 Vine St., Lincoln, NE 68583-0856		10. Work Unit No. (TRAIS)	
		11. Contract or Grant No. 26-1121-4034-001	
12. Sponsoring Organization Name and Address  Nebraska Department of Transportation (NDOT) 1400 Highway 2, PO Box 94759, Lincoln, NE 68509		13. Type of Report and Period Covered  7/1/2016 – 3/31/2018	
		14. Sponsoring Agency Code	
15. Supplementary Notes			
16. Abstract In an effort to improve mechanical properties of asphalt concrete, an exploratory research using mixture additives was attempted. Two different types of additives on two material scales were used: asphalt concrete (AC) level and binder level. At the start of this study, the effect of natural cornhusk fibers on the resistance of two types of AC mixtures on cracking were tested for hot-mix asphalt (HMA) and cold-mix asphalt (CMA). The results showed slight improvements in cracking resistance in cornhusk reinforced HMA, and in the case of the CMA, marshal flow. Overall, based on the test results, cornhusk-reinforced HMA and CMA may not significantly improve critical mechanical properties given the added cost of fibers. In addition, cornhusk fibers proved difficult to properly disperse in HMA and CMA when mixed in laboratory. However, when fibers were mixed in an asphalt production plant, the fibers appeared to become more distributed. The second part of this study, two different types of carbon nano-fillers (F1 and F2) with different surface properties and sizes were added to two different asphalt binders: the base binder and the polymer modified binder. Also, mastic samples were prepared by replacing parts of the limestone filler by the carbon nano-fillers. It was observed that the nanoscale additives interacted with the binder quite differently. Additive F1 did not show a drastic improvement in the mechanical properties, fatigue resistance, and rutting resistance of the base and polymer modified binder at the mastic and the binder scale; however, additive F2 improved all the above-mentioned properties. From the experimental investigation, it can be inferred that part of the polymer modification can be replaced by additive F2. Although additive F1 showed a minimal change, it could be useful in improving the secondary application of the pavement, such as the electrical conductivity, thermal conductivity, and absorption of radiation for energy storage, which was not the scope of this study but appears worthy to investigate.			
17. Key Words Asphalt, Fibers, Nano-fillers	18. Distribution Statement		
19. Security Classification (of this report) Unclassified	20. Security Classification (this page) Unclassified	21. No. of Pages 67	22. Price

## Table of Contents

List of Figures .....	iii
List of Tables .....	vi
Acknowledgements .....	vii
Disclaimer .....	viii
Abstract .....	ix
Chapter 1 Introduction .....	1
1.1. Research Objectives .....	3
1.2. Research Methodology .....	4
1.3. Organization of Report .....	6
Chapter 2 Literature Review .....	7
2.1. Natural and Synthetic Fibers .....	7
2.1.1. Natural Fibers .....	7
2.1.2. Synthetic Fibers .....	8
2.2. Fibers-Reinforced Bituminous Mixtures .....	8
2.2.1. Hot Mix Asphalt .....	8
2.2.2. Cold Mix Asphalt .....	10
2.3. Carbon Nano-fillers .....	10
2.3.1. Carbon Nanotubes (CNT) and Carbon Nanofibers (CNF) .....	10
2.3.2. Nano-Clay (NC) Particles .....	11
2.3.3. Graphite Nano-particles .....	12
Chapter 3 Materials, Testing Facility, and Sample Fabrication .....	13
3.1. Materials for Fiber Reinforced Asphalt Concrete .....	13
3.1.1. Fibers .....	13
3.1.2. Hot-Mix Asphalt .....	15
3.1.3. Cold-Mix Asphalt .....	16
3.2. Materials for Asphalt Binder Modification .....	17
3.2.1. Binder .....	17
3.2.2. Mastic .....	19

3.3. Testing Facility .....	19
3.3.1. Testing Equipment for Fibers .....	19
3.3.2. Testing Equipment for Asphalt Concrete Mixtures .....	20
3.4. Sample Fabrication .....	21
3.4.1. Asphalt Concrete Mixtures .....	21
3.4.2. Asphalt Binder Samples .....	24
Chapter 4 Test Results and Discussions.....	26
4.1. Cornhusk Fibers .....	26
4.2. SCB Test Results of HMA with Cornhusk Fibers .....	28
4.3. SCB Test Results of HMA with Synthetic Fibers .....	31
4.4. Comparison Between Fibers.....	34
4.5. CMA Test Results.....	37
4.5.1. Workability Test .....	37
4.5.2. Marshall Stability-Flow Test .....	38
4.6. Nano-filler Modified Asphalt Binder and Mastic.....	41
4.6.1. Preliminary Investigation .....	41
4.6.2. Primary Investigation .....	46
Chapter 5 Conclusions .....	63
References .....	64

## List of Figures

Figure 1: Asphaltic materials at different length scales: (a) asphalt concrete, (b) fine aggregate matrix (FAM), and (c) asphalt binder or mastic (with fillers). .....	2
Figure 2: Research methodology used for: (a) hot mix asphalt, and (b) cold mix asphalt. ....	5
Figure 3: Research methodology used for nano-sized particles in asphalt cement and mastic.....	6
Figure 4: Cornhusk fibers fabrication scheme.....	14
Figure 5: Cornhusk fibers at different length scales (a) macroscale (average length of 15 mm) and (b) microscale morphology. ....	15
Figure 6: SEM image of nanostructured graphite-250 used in the preliminary investigation. ....	18
Figure 7: Tensile testing of fibers. ....	20
Figure 8: Fabrication of SCB specimen: (a) after compaction, (b) slicing and (c) notching. ....	21
Figure 9: Sample fabrication for Marshall testing: (a) compactor, (b) samples after compaction. ....	22
Figure 10: Cold patch slump test for workability test set-up: (a) by Chatterjee, Smit et al. (2005) (b) used in here. ....	23
Figure 11: Weight loss of cold mix asphalt at 140°F.....	24
Figure 12: Nano-filler and mixing method: (a) nanostructured graphite-250 that was used in the preliminary investigation, (b) Silverson high shear mixer with the aluminum container and heater. ....	25
Figure 13: A typical stress-strain curve of cornhusk fiber. ....	26
Figure 14: Mechanical properties of untreated fibers after 30 minutes exposure at different temperatures. ....	27
Figure 15: Influence of time spent at high temperature (160°C) on tensile properties of fibers...28	
Figure 16: SCB test results at different content of 10-mm fiber: (a) control mixture, (b) 0.1 percent fiber content, (c) 0.2 percent fiber content, and (d) average of replicates. ....	29
Figure 17: SCB test results at different content of 20-mm fiber: (a) control mixture, (b) 0.1 percent fiber content, (c) 0.2 percent fiber content, and (d) average of replicates. ....	30
Figure 18: 20 mm fiber clogging at 0.2 percent fiber content.....	31

Figure 19: Comparison between natural and synthetic fibers during sample fabrication: (a) cornhusk fibers, (b) ACE Fiber™, (c) mixing of cornhusk fibers, (d) mixing of ACE Fiber™, and (e) compacted tall samples. Note: all fibers shown in this figure were 45-mm in length. ....	32
Figure 20: Load vs. displacement test results of 45-mm long fibers mixed and compacted at different locations: (a) UNL laboratory and (b) prepared at an asphalt production plant. ....	34
Figure 21: Calculated fracture parameters from test results with standard deviation as error bars: (a) fracture energy, (b) flexibility index. ....	36
Figure 22: Results from workability test of 20 mm fibers at 0.3percent content. ....	37
Figure 23: Typical Marshall test results showing force vs load point displacement (LPD). ....	38
Figure 24: Test results of fiber reinforced cold mix: (a) Marshall flow, (b) Marshall stability. ...	39
Figure 25: Failure of cold mixes (a) Permapatch (material failed shortly after compaction and before testing), (b) QPR material 24 hours after testing showing coherent samples with long fibers. ....	40
Figure 26: Master curve for base binders and its modified form formed by adding different dosage of NG-250 carbon filler to B and P (a) $ G^* $ values vs frequency (b) $\delta$ values vs frequency. ....	42
Figure 27: Strain sweep data at 0 °C and 40 °C at frequency 0.1 and 10 Hz for PG64-34 binder and its nanofiller modified binder at a dosage of 1.0 percent. ....	43
Figure 28: Temperature sweep: (a) storage and loss modulus, and (b) phase angle for 8 mm and 25 mm parallel plate of base binder. ....	44
Figure 29: Temperature sweep for base binder (a) storage and loss modulus (b) phase angle at different frequencies. ....	45
Figure 30: Master curves for base binder and its nano-modified binder using fillers F1 and F2 at a dosage of 15 percent and 25 percent; the polymer modified PG 64-34 is shown for comparison. ....	49
Figure 31: Master curve for polymer modified PG 64-34 and its corresponding nano-modified binder using nano-filler F1 or F2 at a dosage of 10 percent; also included is the base binder modified with nano-filler F2 (15percent).....	50

Figure 32: Mastic master curves for base binder modified by limestone filler and its corresponding nano-modified mastic samples.....	51
Figure 33: Mastic master curve plots for base binder mastic, polymer modified mastic, and its corresponding nano-modified mastics. ....	51
Figure 34: Amplitude sweep results for base binder PG49-34 and its nanomodified binder by fillers F1 and F2 at (a) 20 °C (b) 10 °C. ....	52
Figure 35: Amplitude sweep results for mastic samples for PG64-34+LS and its modified mastic obtained by replacing part LS by F1 and F2 at 20 °C & 10 °C. ....	53
Figure 36: MSCR test results for polymer modified binder and its nano-modified binders (a) 64°C, (b) 70°C, and (c) 76°C.....	55
Figure 37: MSCR test result for P at 64 °C and B+F2(15%) case at 50 and 64 °C.....	56
Figure 38: MSCR test results for base mastic and its nanomodified samples prepared by replacing part of the LS (a) 64°C, (b) 70°C, and (c) 76°C.....	58
Figure 39: Temperature sweep results for binder showing (a) $G'$ , $G''$ , and $\delta$ vs temperature, and (b) normal force vs temperature. ....	59
Figure 40: Temperature sweep results for base binder, polymer modified binder, and its nano-filler modified forms using filler F1 and F2: (a) $ G^* $ vs temperature, (b) $\delta$ vs temperature. .	61
Figure 41: Temperature sweep results for base polymer modified binder and its mastic forms modified with filler F1 and F2 (a) $ G^* $ vs Temperature (b) $\delta$ vs Temperature. ....	62



## List of Tables

Table 1: Characteristics of Fibers .....	7
Table 2: Mixture Properties and Aggregate Gradation of HMA .....	16
Table 3: Aggregate Gradations of Cold Mixes .....	16
Table 4: Properties of Nanostructured Graphite-250 .....	18
Table 5: Properties of the Carbon Nano-fillers Used in This Study .....	19
Table 6: Test Samples with Different Dosage and the Tests Conducted on These Samples as Part of the Preliminary Investigation .....	41
Table 7: Notations Used to Represent the Binder Samples Prepared in the Current Study .....	47
Table 8: Notations Used to Describe the Mastic Samples Prepared in the Current Study .....	48

## Acknowledgements

The authors would like to thank the Nebraska Department of Transportation (NDOT) for the financial support needed to complete this study. In particular, the authors thank the NDOT Technical Advisory Committee (TAC) for their technical support and their invaluable discussion and comments.

## Disclaimer

The contents of this report reflect the views of the authors, who are responsible for the facts and the accuracy of the information presented herein. This document is disseminated under the sponsorship of the U.S. Department of Transportation's University Transportation Centers Program, in the interest of information exchange. The U.S. Government assumes no liability for the contents or use thereof.

## Abstract

In an effort to improve mechanical properties of asphalt concrete, an exploratory research using mixture additives was attempted. Two different types of additives on two material scales were used: asphalt concrete (AC) level and binder level. At the start of this study, the effect of natural cornhusk fibers on the resistance of two types of AC mixtures on cracking were tested for hot-mix asphalt (HMA) and cold-mix asphalt (CMA). The results showed slight improvements in cracking resistance in cornhusk reinforced HMA, and in the case of the CMA, marshal flow. Overall, based on the test results, cornhusk-reinforced HMA and CMA may not significantly improve critical mechanical properties given the added cost of fibers. In addition, cornhusk fibers proved difficult to properly disperse in HMA and CMA when mixed in laboratory. However, when fibers were mixed in an asphalt production plant, the fibers appeared to become more distributed. The second part of this study, two different types of carbon nano-fillers (F1 and F2) with different surface properties and sizes were added to two different asphalt binders: the base binder and the polymer modified binder. Also, mastic samples were prepared by replacing parts of the limestone filler by the carbon nano-fillers. It was observed that the nanoscale additives interacted with the binder quite differently. Additive F1 did not show a drastic improvement in the mechanical properties, fatigue resistance, and rutting resistance of the base and polymer modified binder at the mastic and the binder scale; however, additive F2 improved all the above-mentioned properties. From the experimental investigation, it can be inferred that part of the polymer modification can be replaced by additive F2. Although additive F1 showed a minimal change, it could be useful in improving the secondary application of the pavement, such as the electrical conductivity, thermal conductivity, and absorption of radiation for energy storage, which was not the scope of this study but appears worthy to investigate.

## Chapter 1 Introduction

Asphalt concrete (AC) is the most commonly used road paving material in the United States (U.S). The primary function of the asphalt pavement can be defined as a structure that is safe, reliable and can provide a comfortable means for transportation, resist mechanical and environmental loads, and is sustainable and ecofriendly. In the U.S, domestically, in 2015, freight worth over 15 trillion were moved using several transport modes, among which a large portion of 73 percent were moved by trucks on roads (Michael J. Sprung 2017). In the same year, among a total of 948,165 paved road miles, about 82 percent were paved using AC, which to about 60 percent of all road freight were moved on roads paved in AC (FHWA 2015). With a projected increase in population, a reliable and sustainable transportation and roadway system is a necessity to accommodate the associated increase in vehicle miles of travel (VMT). Therefore, it is imperative to perpetually improve the performance of AC pavements.

Among others, AC performance can be improved by incorporating additives that compensate for lacking properties such as high cracking resistance in AC and better raveling resistance in cold mixes. In addition, nano-sized particles can be used to modify asphalt binder with the aim of ameliorating its mechanical properties and thus that of AC.

Fundamentally, AC is made of a combination of aggregates and asphalt cement (binder). The binder is a viscous material that acts as a glue holding the rigid aggregates together. In this sense, aggregates act as an elastic component while the asphalt binder serves as a viscoelastic component, resulting in a viscoelastic AC mixture. Due to the discrete nature of the aggregates, AC exhibits better resistance in compression rather than tension, rendering it vulnerable to failure from tensile loading. Failure in AC is manifested in several forms, such as thermal and fatigue cracking and raveling. To tackle this issue and others, improved material and mixture systems need to be developed toward increasingly more engineered, sustainable, economical, and better-performing infrastructure.

The improvement of the performance of AC can be achieved through different approaches (i.e., pavement design or material design), both of which have a significant outcome on the sustainability of road structures. This study attempted to improve material properties by using innovative, new, and economical additive materials. A multiple length-scale approach was

employed in which two types of additives were used to modify properties of asphaltic materials at different length scales such as: AC and asphalt binder (cement). On the first length scale, fibers (e.g., cornhusk fibers) were used with the goal of improving tensile fracture properties on the AC scale (Figure 1 (a)). On the binder length scale, carbon nano-fillers were used to modify asphalt binder (Figure 1 (c)) with the goal of improving high and low temperature mechanical properties of the binder and thus ultimately, those of the entire AC mixture. Figure 1 shows three conceptual length scales of asphaltic materials. The first is the AC scale, which is inclusive of all components. The second length scale, called fine aggregate matrix (FAM), which excludes aggregates larger than 1.19 mm (#16 sieve) (Im et al. 2014), while asphalt cement mixed with particles passing # 200 sieve (mesh size of 0.075 mm) is considered asphalt mastic (scale III).

Addressing problems in AC, such as cracking due to a lack of resistance to tensile loading can be achieved through reinforcement of internal structure. In AC mixtures, such reinforcement can be made by adding fibers that serve as tensile stress resisting components. Several studies have attempted to use synthetic fibers with varying outcomes (Lee et al. 2005, Tapkın 2008, Xu et al. 2010, Dehghan et al. 2017) and natural fibers (Gallo 2017).

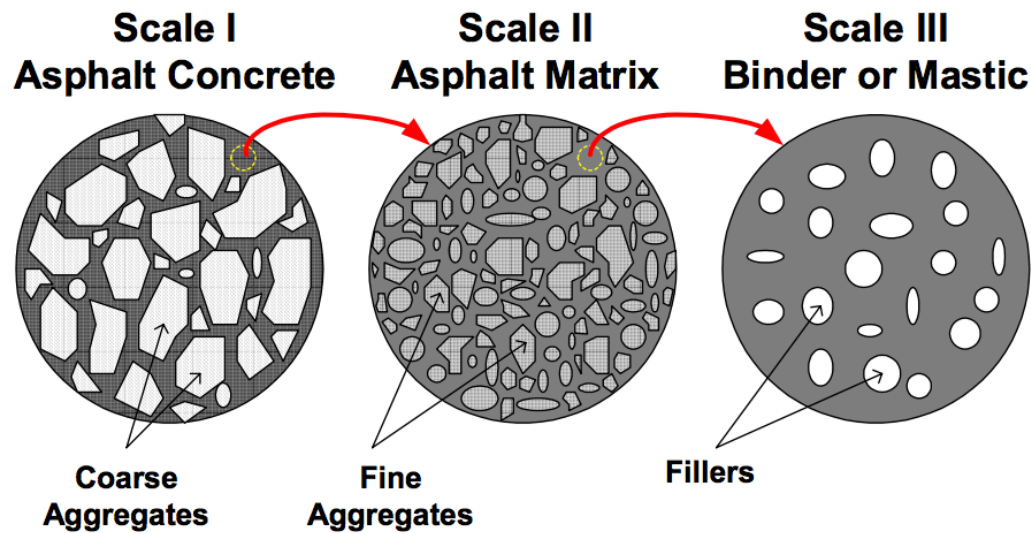


Figure 1: Asphaltic materials at different length scales: (a) asphalt concrete, (b) fine aggregate matrix (FAM), and (c) asphalt binder or mastic (with fillers).

As a by-product from corn production in Nebraska, cornhusk is largely available and inexpensive. Cornhusk fibers can be extracted to produce textiles, composites, and filters (Reddy et al. 2005), and showed good reinforcing effects in composites with synthetic and natural matrices (Reddy et al. 2009). In addition, due to their good biodegradability, cornhusk fibers could be prospective fiber candidates in many applications. Considering the increased significance of sustainability in pavement engineering, cornhusk fibers could be a suitable candidate for asphalt mixtures, and were thus selected as fiber reinforcements in this research.

In addition to only focus on improving the structural function of AC, current trends in pavement design and engineering focus on non-structural functions or the secondary functions of pavements (Liu et al. 2011, Rew et al. 2017, Sun et al. 2017). The aforementioned reinforcement can also be implemented on a lower length scale such as the FAM and asphalt mastic/cement length scale. This is typically done by adding binder modifiers such as polymers (Yildirim 2007) to improve binder grade, and by adding nano-sized particles to primarily improve properties. For example, the addition of nanoparticles to AC mixtures could indirectly have a positive contribution to structural functioning through the improvement of secondary functions (Lu et al. 2015). Diverse types of nanomaterials have been attempted to asphalt binders. The addition of nanoparticles to improve the primary function has been quite indispensable due to improved performance in many perspectives (Lu, Xie et al. 2015). Over the past few decades, researchers have focused on improving the primary function of the asphalt composite structure.

Although the effects of the modification by adding nano-sized particles can be experimentally analyzed at different length scales such as binder, mastic, FAM, and AC, the modifiers are mostly added to the binder as additives. This study, as a parallel effort to the aforementioned fiber reinforcement in AC level, investigated the effects of nano-sized particles on binder and mastic phase. Two different nano-sized fillers were selected to modify the binder and mastic phase, and their contributions were evaluated by mechanical and chemical tests-analyses.

### 1.1. Research Objectives

This research is to seek exploratory mixture additives for more sustainable bituminous mixtures. Two different types of additives on two material scales were used: asphalt concrete (AC) level and binder/mastic level. On the AC scale, locally available natural cornhusk fibers were explored as

potential reinforcing materials to modify AC. On the binder/mastic length scale, nano-sized particles were used as modifiers/fillers. Two specific objectives of this research are:

- To evaluate the feasibility of using abundant natural fibers in Nebraska (i.e., cornhusk fibers) as reinforcing material in hot mix and cold mix AC.
- To characterize mechanical and chemical properties of nano-sized particles in asphalt cement and mastic to improve entire AC mixtures.

## 1.2. Research Methodology

To meet the first objective, the compatibility of cornhusk fibers and AC was first investigated by characterizing mechanical properties (e.g., tensile strength) of fibers subjected to increasing temperatures ranging from room temperature to 160°C. Second, the effect of the amount of time spent (e.g., from 0 to 2 hours) at high temperatures (i.e., 160°C) on fibers was investigated. Subsequently, fibers were mixed with an AC mixture in the laboratory to produce fiber-reinforced asphalt concrete (FRAC). The fiber reinforcing effect on two types of AC mixtures, hot mix asphalt (HMA) and cold mix asphalt (CMA), was assessed. In the HMA, the semicircular bend (SCB) fracture test (Nsengiyumva 2015) was used to characterize the contribution of fibers on the fracture properties of HMA-FRAC, while the CMA mixtures were evaluated by performing the Marshall test (ASTM D6927 - 15). The methodology is illustrated in Figure 2. Finally, natural fibers are compared to synthetic fibers used in HMA-FRAC for their relative performance.



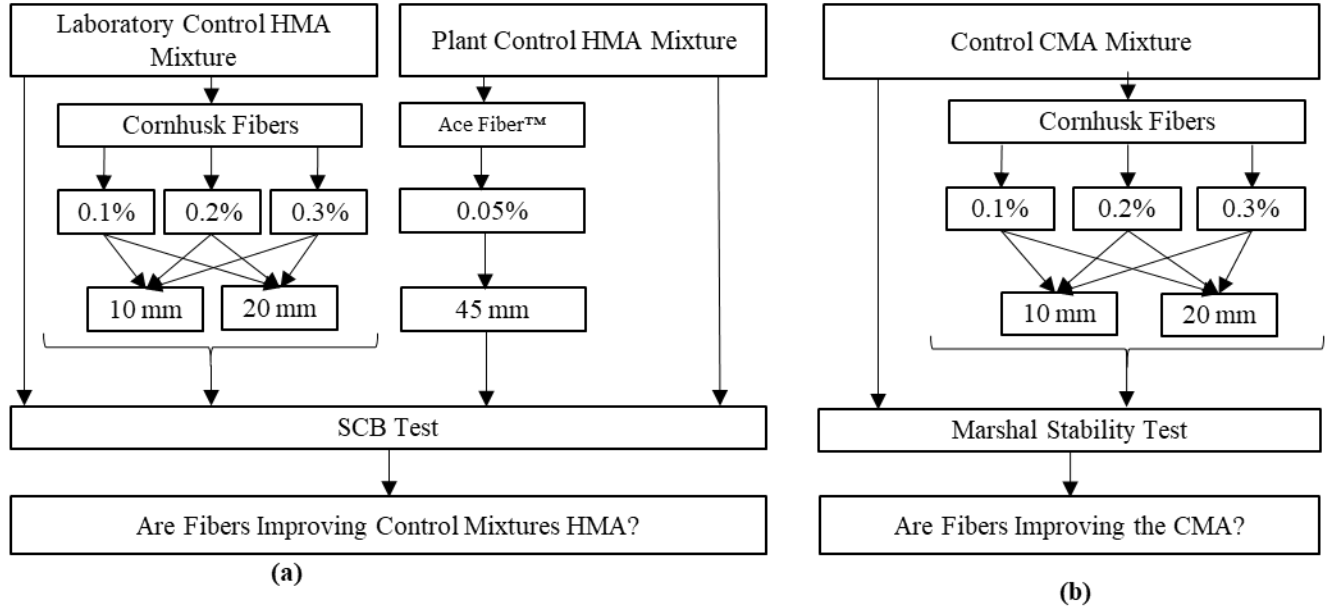


Figure 2: Research methodology used for: (a) hot mix asphalt, and (b) cold mix asphalt.

For the second part of this study, the influence of nano-fillers on the rheological properties of the binder was investigated. Two different types of nano-fillers were selected to be added to the base binder PG 49-34 and its polymer-modified form PG 64-34. Similar investigation was also carried out for the mastic samples prepared by using the aforementioned binders and limestone mineral fillers. The nano-modified mastics were prepared by replacing parts of the limestone filler with the carbon based nano-fillers. Figure 3 shows the research methodology and scope of the second part of the study.

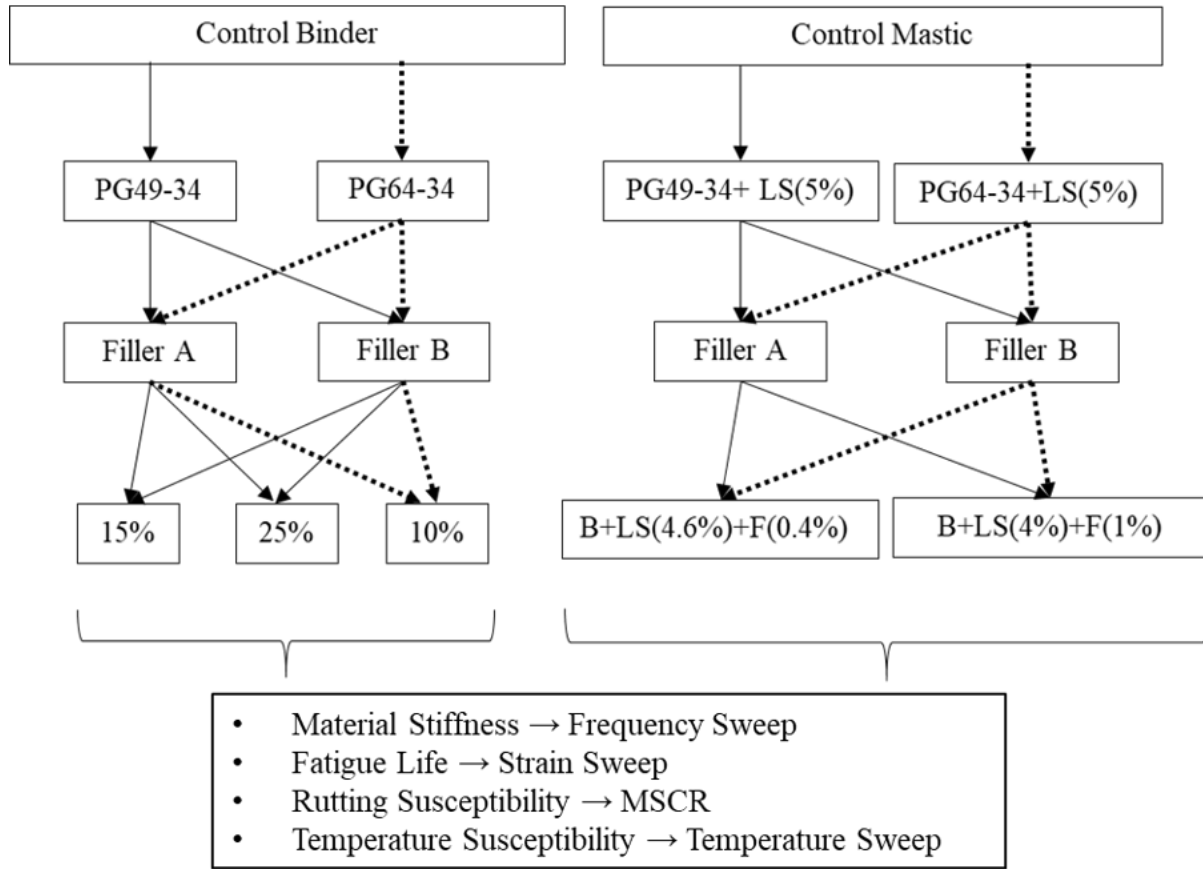


Figure 3: Research methodology used for nano-sized particles in asphalt cement and mastic.

### 1.3. Organization of Report

This report is organized in five chapters. The first chapter introduces this research effort and its importance with a brief literature perspective, then the research objectives and methodology. The second chapter summarizes relevant literature grouped in two main parts related to each length scale: fibers (i.e., natural and synthetic) for AC scale and nano-sized carbon modifiers/fillers for binder/mastic scale, respectively. In the third chapter, materials and their properties are presented along with the testing facility and test setups. In the following chapter, test results and discussions are presented. In chapter five, important findings and conclusions drawn from this research are presented.

## Chapter 2 Literature Review

A literature review is presented in this chapter. First, literature on natural fibers is examined, with a focus on cornhusk fibers and their advantages compared to other types of natural fibers. Then, literature summarizing studies conducted on mainly natural fibers in HMA and CMA is presented. Finally, relevant research on nano-sized fillers in asphalt cement are presented. Key findings from the literature review are summarized at the end of this chapter.

### 2.1. Natural and Synthetic Fibers

#### *2.1.1. Natural Fibers*

Natural fibers are extract from plants and are composed of cellulose, hemicellulose and lignin intricately arranged in layers around a lumen core to give the fiber the necessary strength to withstand force. However strong, the layers in natural fibers are porous and thus relatively higher moisture absorbent compared to synthetic fibers. As evident from Table 1 which exemplifies key characteristics of natural fibers (e.g., cornhusk), and synthetic fibers (e.g., polyester and nylon 6), moisture regain of natural fibers is significantly higher than synthetic fibers. Furthermore, Table 1 shows lower tensile strength of the natural fiber compared to synthetic fibers while the elongation at breaking was relatively similar for all fibers. Compared to other types of natural fibers, such as linen and flax fibers, cornhusk fiber is capable of undergoing higher strain levels prior to breakage (Reddy and Yang 2005, Reddy et al. 2007).

Table 1: Characteristics of Fibers

Fiber	Tensile strength (MPa)	Breaking elongation (%)	Moisture regain (%)
Cornhusk	194-262	10.8-13.0	9-10.5
Polyester	536-664	15-35	0.1-0.4
Nylon 6	485-792	18-45	3-5

### *2.1.2. Synthetic Fibers*

Synthetic fibers are usually products of polymerization of smaller components from crude oil. The most common synthetic fibers include: polyester and nylon 6 fibers which are commercially available. Polyester fibers have very low moisture regain, while nylon 6 fibers have 3-5 percent moisture regain due to existence of polar amide groups (see Table 1). Tensile strength and strain of polyester and nylon 6 fibers are both higher than cornhusk fibers. However, the two synthetic fibers are derived from petroleum and are not degradable.

## 2.2. Fibers-Reinforced Bituminous Mixtures

### *2.2.1. Hot Mix Asphalt*

Several studies have sought to improve overall performance of AC by incorporating fibers as means of reinforcement. Both types of fibers, synthetic and natural, have been explored with varying degrees of success.

#### Synthetic Fibers

Most studies on fiber-reinforced AC (FRAC) using synthetic fibers reported an increase in fatigue cracking resistance (Lee, Rust et al. 2005, Kaloush et al. 2010). Lee, Rust et al. (2005) used nylon fibers to reinforce AC after first identifying the optimum length by fiber pull out test which involves pulling a single fiber embedded in asphalt cement at varying lengths. The study found 9.2 mm or longer to be the length at which shear stress at the fiber-asphalt interface equals the maximum tensile strength allowed in fiber, thus allowing maximum contribution from fibers to bridge cracks and limiting the undesired slipping of fibers.

Kaloush, Biligiri et al. (2010) modified a conventional AC by adding one pound of synthetic fibers (mixture of aramid and polypropylene) per ton and investigated changes in key mechanical characteristics such as stiffness, fatigue cracking, and permanent deformation. The study reported improvement in mechanical characteristics of FRAC mixtures when compared to control mixtures. In addition to laboratory tests, field study was conducted. Road sections with FRAC showed no cracks while low severity cracks were observed in the control section.

In open graded mixtures, fibers were reported to reduce drain-downs. Although most synthetic fibers tend to be polymers, several studies (Mahrez et al. (2005), (Chen et al. 2009) attempted to modify stone mastic asphalt (SMA) with glass fibers to increase strength and fatigue

resistance. Later, Chen et al. (2010) studied the effects of several types (i.e., polyesters, polyacrylonitrile, lignin and asbestos) of synthetic fibers on the reinforcement of asphalt concrete. Among other tests conducted in the study, the authors observed the microstructure characteristics of fiber reinforced mixtures and concluded that fibers formed a three-dimensional network in the asphalt binder that would resist cracking and improve stress distribution throughout the mixture.

### Natural Fibers

Beyond synthetic fibers, natural fibers are attractive in that they are biodegradable and readily available from crops and plants. Natural fibers have been recognized by their low-cost, high-tensile strength compared to synthetic fibers (Ahmad et al. 2015), and have been used by multiple industries such as car manufacturing. In the paving materials community, natural fibers such as cellulose are mainly used in asphaltic mixtures for their high absorption to limit drain down of binder in stone matrix asphalt (SMA) (Putman et al. 2004) and open graded friction course (OGFC) (Watson et al. 1998). Recently, Gallo (2017) modified AC with several natural fibers (e.g., hemp, flax, wool, yarn, etc.), and then conducted an indirect tensile test, which concluded that natural fibers may have great potential in improving asphalt concrete.

Mansourian et al. (2016) conducted a series of semi-circular bending (SCB) tests and numerical simulations of warm-mix asphalt (WMA) mixtures reinforced with jute natural fibers at different fracture modes (i.e., opening mode, shearing mode, and mixed mode) by varying fiber content (0.0, 0.3, 0.5 and 0.7%), and testing temperatures (0, -10, -20°C). In the study, it was found that the effect of fiber on fracture properties was more beneficial in the pure opening mode fracture irrespective of fiber content or temperature. In their subsequent study, Aliha et al. (2017) compared jute fibers to synthetic fibers made of polyolefin-aramid by conducting the same SCB fracture testing by varying fracture modes, testing temperatures, and fiber contents. It was noted that, synthetic fibers were coated with polyolefin wax which then melted during mixing and acted as a WMA modifier. Results from the study showed that fracture toughness increased with decreasing temperature. In addition, at all temperatures investigated in the study, at 0.3 percent fiber content, the effective toughness stabilized and was maximum at the pure opening and pure shearing conditions, respectively.

### *2.2.2. Cold Mix Asphalt*

Despite great performance potential, the subject of improving cold mix asphalt (CMA) concrete with fibers (albeit natural or synthetic) is relatively newer than HMA and WMA counterparts and thus the scarcity of studies on this subject. Recently, Shanbara et al. (2017) attempted to explore natural fibers (coconut-husk) and synthetic fibers (glass) as a means of improving mechanical properties of CMA mixtures. Test results showed that the key mechanical characteristics such as stiffness, creep, moisture susceptibility, and rutting did improve when fibers were added irrespective of fiber types. It is noted, however, that the synthetic glass fibers were marginally better than natural fibers except for moisture susceptibility where the synthetic fibers were performed significantly better than natural fibers. This might be due to the high moisture absorption characteristic of natural fibers in general.

## 2.3. Carbon Nano-fillers

### *2.3.1. Carbon Nanotubes (CNT) and Carbon Nanofibers (CNF)*

A study (Ameri et al. 2016) investigated the influence of adding different dosages of CNT's to the mixture to study the fatigue and fracture resistance of the AC by performing SCB and four-point bending beam tests. They observed that the cracking and fatigue resistance improved considerably at higher dosages but did not obtain pronounced changes in these properties at lower dosages of CNT. Another study (Santagata et al. 2015) showed healing capabilities of CNT and montmorillonite nano-clay in the mastic.

Another popular nano-modifier is the carbon nanofiber. It is with a high aspect ratio ( $\approx 1,700$ ). It was observed that the carbon nanofibers have the ability to bridge the cracks developed at the micro-scale (Khattak et al. 2012) and hence improve the fatigue resistance of the asphalt binder. They also observed increased rutting resistance. Based on the above results they conducted several tests on the CNF modified AC (Khattak et al. 2013) to investigate the material properties and evaluate the resistance to fatigue damage. They observed that the dynamic shear modulus ( $|G^*|$ ) and fatigue life improved but that no major difference was obtained in their indirect tensile strengths and fracture toughness. It is clear that the mechanical properties of AC are strongly influenced by the degree of uniform distribution of the nanofibers in the binder phase.

However, there are several disadvantages associated with the use of either the CNF or CNT as modifiers. One is the cost as it is much more expensive compared to using polymers to modify the base binder (Santagata, Baglieri et al. 2015). Also, the difficulty in obtaining a uniform state of dispersion of the fillers in the binder was often reported (Khattak, Khattab et al. 2013, Lu, Xie et al. 2015, Santagata, Baglieri et al. 2015).

### *2.3.2. Nano-Clay (NC) Particles*

Several researchers (Ghile (2006), Jahromi et al. (2009) have worked on modifying the binder using organic nano-clay particles as they are naturally occurring minerals and cause no environmental damage. More recently, Yao et al. (2015) studied changes in the major chemical groups such as ketones, aldehydes, anhydrides, esters, and carboxylic acid when asphalt binder was aged in short and long term conditions in the presence of montmorillonite nano-clay particles. Another group of researchers (Wu et al. 2010, Liu et al. 2011) performed experimental studies in the fatigue resistance of a nano-clay modified binder. They indicated that the level of interaction between the binder and the nano-clay particles at the interface plays a major role in enhancing the fatigue life of the mixture. One of the most popular usages of nano-clay particles can be found in the modification of polymer-based binders. The clay particles are able to interact with polymer matrix by forming a strong network. Even at relatively small dosages of nano-clay addition, significant amounts of improvement in mechanical, thermal, and aging resistance of the binder was observed (Jahromi and Khodaii 2009, You et al. 2011). Researchers have also confirmed that interaction at the nanoscale between nano-clay and binder could be achieved given that the clay particles are exfoliated and dispersion occurs at the nano-level. This would require a specific type of blending procedures to be used, which use additional surfactants to separate the clay layers. Test results have also shown that nano-clay can enhance physical and rheological properties of the polymer modified asphalt binder as well as its storage stability. With these enhanced binder characteristics, the asphalt concrete specimens showed an increase of tensile strength and resilient modulus and also improved rutting resistance over conventional asphalt concrete (Golestani et al. 2015).

### *2.3.3. Graphite Nano-particles*

Many different types of nano-modifiers are available, and it would be beyond the scope of the current investigation to include all of them. Based on the literature review, two important aspects are to be considered: one is cost effectiveness as adding nano-filler can increase production cost significantly, and secondly, the multifunctional feasibility of the mixture due to the addition of nano-filler. Graphite nano-powders can satisfy both aspects.

Addition of graphite to asphalt binder has been of interest to researchers due to its high thermal and electrical conductivity. The main idea is to improve the conductivity of the asphalt concrete such that the structure could be used for multiple purposes as a smart pavement. The goal has been to make the asphalt concrete a self-monitoring structure that can assist in multiple functions such as deicing, self-healing, self-monitoring of strain-stress behavior, and improving the electrical conductivity (Pan et al. 2015). Different types of nano-filler have been used to make the asphalt concrete a conductive material. The addition of nano-filler to improve the conductivity is being investigated by many researchers. This is mostly to use cost effective substitutes for graphene nanoplatelets (GNP), which can be expensive for a large usage such as pavement construction. Adding flake type graphite powders at low concentrations of 2-3 percent by volume of asphalt concrete could improve the conductivity of the system (Rew, Baranikumar et al. 2017).



## Chapter 3 Materials, Testing Facility, and Sample Fabrication

In this chapter, materials and testing facility used in this project are presented. At the end of the chapter, sample fabrication is explained for all materials investigated here.

### 3.1. Materials for Fiber Reinforced Asphalt Concrete

#### *3.1.1. Fibers*

Fibers were obtained from cornhusks via a combined chemical and enzymatic extraction process. Cornhusks were treated with 0.5 N sodium hydroxide solution for 60 minutes at 95 °C with 5 percent of the cornhusks, according to weight, in the alkali solution to remove hemicellulose, lignin, and other compositions. The treated slurry was washed in water to remove the dissolved substances and the fibers obtained were neutralized using 10 volume/volume (v/v) percent acetic acid solution. The neutralized fibers were dried under ambient condition and combed and cut into required lengths (5 mm, 10 mm, 20 mm, etc.). Figure 4 shows the entire process of preparation of cornhusk fibers.

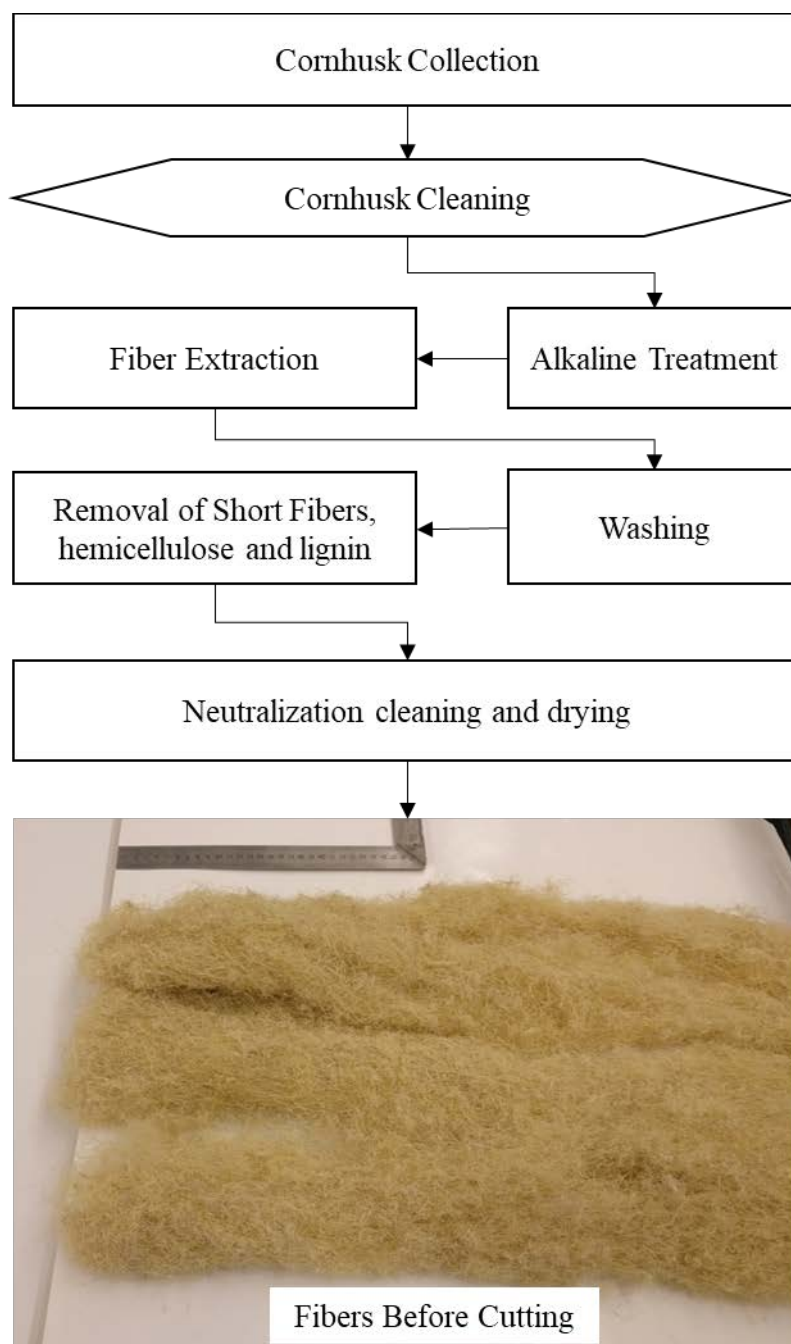


Figure 4: Cornhusk fibers fabrication scheme.

After the fabrication, the yellow appealing cornhusk fibers were then cut down into desired length (e.g., 10mm, 20 mm, etc.) (Figure 5(a)). Further on a microscale level scanning electron microscope SEM image reveals multiple spiky ends of micro-fibrils extruding from the fibers

(Figure 5(b)). It is hypothesized that this particularly rough surface of the fibers might strengthen asphalt-fibers interphase by increasing contact area.

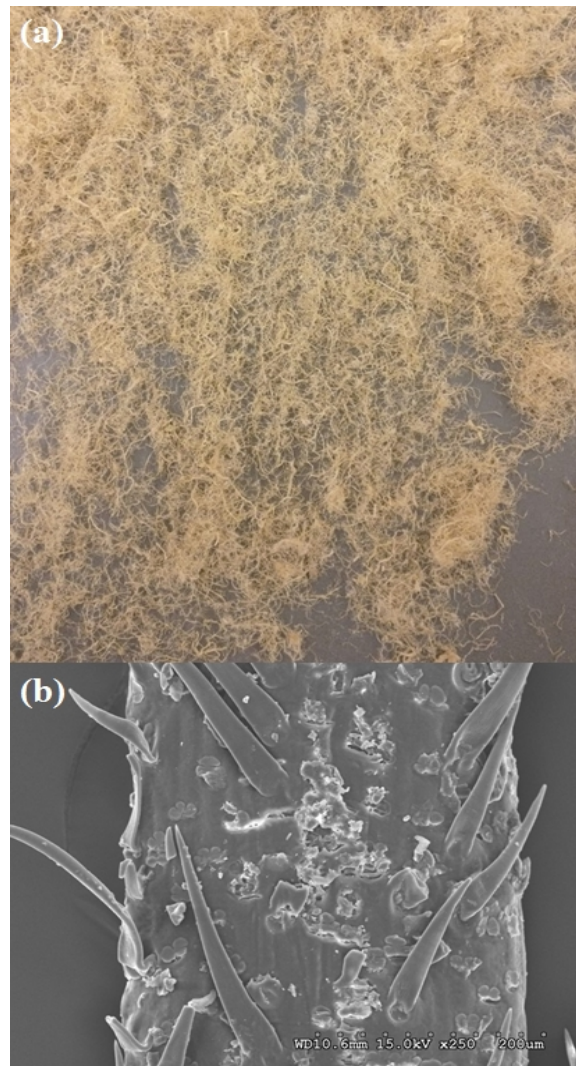


Figure 5: Cornhusk fibers at different length scales (a) macroscale (average length of 15 mm) and (b) microscale morphology.

### 3.1.2. Hot-Mix Asphalt

The asphalt concrete mixture used was a typical Nebraska mixture (SPR) used generally as a surface mix. The mixture was transported in a sealed container from the mixing plant to the Materials Laboratory at University of Nebraska-Lincoln (UNL). Table 2 shows the SPR mixture properties and aggregate gradation.

Table 2: Mixture Properties and Aggregate Gradation of HMA

Mix Type	SPR (Warm Mix Asphalt)											
Binder Source & Grade	MONARCH 64-34 W/0.7% Evotherm											
Compaction Temperature	290°F											
Bulk Specific Gravity (Gsb)	2.585											
Aggregate Gradation (crushed Limestone)												
Sieve Size %	1"	3/4"	1/2"	3/8"	# 4	# 8	#16	#30	#50	#100	# 200	
Passing	100	100	96.9	93.5	80.1	51.2	34	22.7	13.7	8.7	6.2	

### 3.1.3. Cold-Mix Asphalt

To investigate the effect of fibers on differently graded cold mixes, two commercially available mixtures typically used in Nebraska were chosen. The two mixes represent two categories of cold mixes: uniformly graded and open graded mixture. Although both mixtures are commercially available, cold mixes were supplied to testing labs at UNL by the Nebraska Department of Transportation (NDOT) in closed and sealed buckets containing sample materials from production plants. The main differences between the two mixtures were gradation and the emulsified asphalt cement used. The first material, QPR, contained aggregates which are more uniformly distributed compared to the second mixture (Permapatch) as presented in Table 3. Both materials contained emulsified proprietary binders that allowed easy workability at low temperatures (e.g., -15°F).

Table 3: Aggregate Gradations of Cold Mixes

Sieve Sizes	QPR (QPRUSA 2014)	Permapatch (MacAsphalt)
3/8"	100-100	90-100
# 4	20-85	30-75
# 8	2-30	5-30
#16	0-10	0-10
#50	0-6	0-2
# 200	0-2	-

Note: '-' means not specified

## 3.2. Materials for Asphalt Binder Modification

### *3.2.1. Binder*

For the current investigation, two types of binders were selected: one is the base binder and the other is the polymer-modified form derived from the same base binder. The choice of the binder was such that one can assess the influence of nano-filler in the presence and absence of polymer. The nano-fillers could interact with the polymer chain more than that of the matrix of the binder. The base binder is usually the crude/direct form of the binder that was received from the refineries which met the PG 49-34 or a PG 49-28 true grading of the binder performance grade; the later grade is more widely used in the state of Nebraska. The base binders are later modified by adding polymer to meet the necessary performance grade requirement for pavement construction. The current base binder was received from Flint Hills meeting a PG 49-34 true grade. This binder was modified by adding 4 percent by weight of styrene butadiene styrene (SBS) polymer to meet the PG 64-34 grade.

### *3.2.2. Carbon Nano-filler*

There are several choices for the nano-modification of the binder based on the literature review; however, to meet the scope of this project, nano-graphite particles were selected to add as fillers to the binders. Initially, to conduct a preliminary investigation on the effect of adding graphite particles, nanostructured graphite-250 obtained from Graphene Factory was used. Figure 6 shows the scanning electron microscope (SEM) image of the graphite particles, and Table 4 shows the properties of the nanostructured graphite-250.

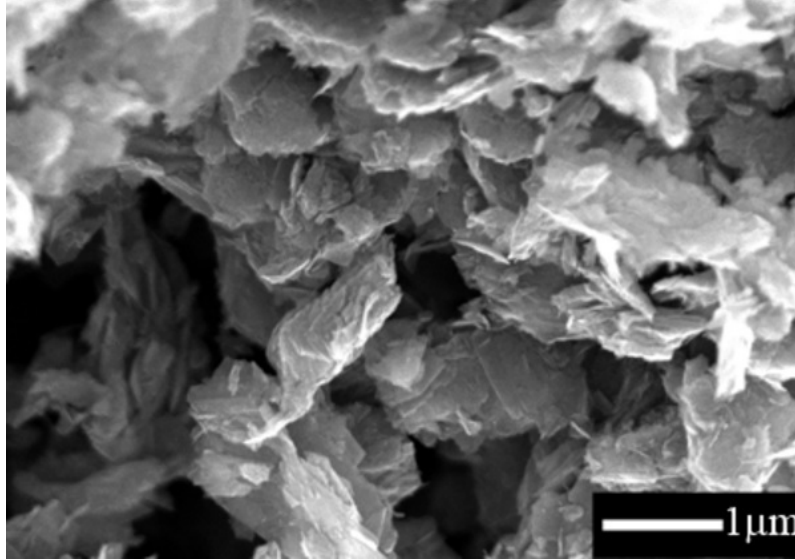


Figure 6: SEM image of nanostructured graphite-250 used in the preliminary investigation.

Table 4: Properties of Nanostructured Graphite-250

Specific Surface Area	250 [m <sup>2</sup> /g]
Lateral Size	100-500 [nm]
Thickness	100-300 [nm]
Bulk Density	0.4 [g/cm <sup>3</sup> ]
Real Density	2.2 [g/cm <sup>3</sup> ]

Based on the outcomes from the preliminary results which are discussed in a later chapter, two nano-fillers (i.e., Graphite TC307 and Carbon Black CB5303) were selected for the remainder of investigation, and their properties are presented in Table 5. It should be noted that the cost of SBS polymer is around \$1,500 per ton which is \$0.75 per pound which is currently a much cheaper option than carbon nano-material modification.

Table 5: Properties of the Carbon Nano-fillers Used in This Study

Material	Asbury ID	Percent Carbon	Typical Size ( $\mu\text{m}$ )	True Density	Surface Area ( $\text{m}^2/\text{g}$ )	Typical Resistivity ( $\Omega\cdot\text{cm}$ )	TL Price (\$/lb)	Note
Graphite	TC307	99.92	< 1 $\mu\text{m}$	2.2	352	0.289	\$4.58	Artificial graphite nanoplatelet
Carbon Black	CB5303	99.9	0.03	1.8	254	0.341	\$7.87	Carbon black

### 3.2.2. Mastic

In asphalt concrete, the fine particles which are usually less than 75  $\mu\text{m}$  in size are present in the form of dust particles. These particles, typically called fillers, enter into the mixture during onsite production of the asphalt concrete mixture. The state of Nebraska requires the dust to binder ratio to be in the range of 0.7 to 1.7 to mitigate inadequate binder thickness that could result in reduced instability or reliability of the AC (DOT 2004). In this study, a dust to binder ratio of 1.0 was considered to prepare the mastic samples for both the control case and carbon filler modified case. For the control case, 50 percent by weight of the mastic was binder and the other 50 percent was composed of limestone filler. For preparing the carbon modified case, a portion of the limestone filler was replaced by the carbon nano-filler to evaluate the influence and behavior of the carbon fillers in the presence of other natural mineral fillers. The mastic samples were prepared by heating the binder and the fillers to 150 °C in separate small containers, and then mixed manually till a uniform distribution of the blend was achieved.

## 3.3. Testing Facility

### 3.3.1. Testing Equipment for Fibers

All fibers to be tested were conditioned in a standard testing environment with a temperature of 21 °C and relative humidity of 65 percent for 24 hours before testing. Tensile properties of fibers were determined with an Instron 4400 tensile testing machine (Instron Co., Canton, MA) according to ASTM D3822 (Figure 7). A load cell of 5 Newton was used to determine the tensile strength, breaking elongation and Young' modulus of the cornhusk fibers. The gauge length was 25 mm,

and the cross-head speed was 18 mm/min. For each sample, about 50 specimens were tested, and the average and standard deviation were recorded.

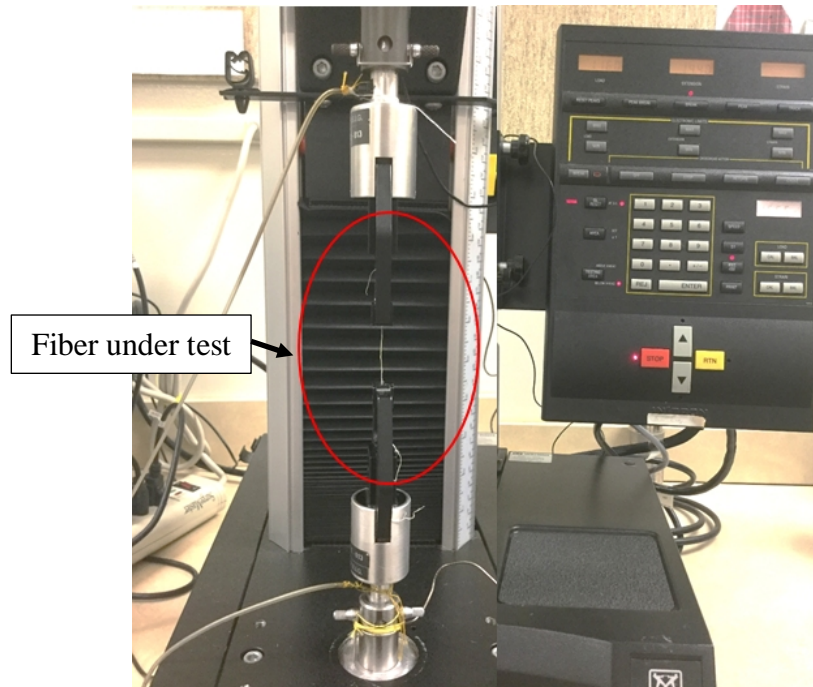


Figure 7: Tensile testing of fibers.

### 3.3.2. Testing Equipment for Asphalt Concrete Mixtures

Mechanical testing of asphalt concrete mixtures, for both HMA and CMA, were conducted using a UTM-25kN testing equipment. The testing station was also equipped with an environmental chamber capable of maintaining temperatures between -16 °C to 60 °C, and a load cell with the capacity of 25kN. A hydraulic system supplied necessary loading force while loading and acquisition control were performed by a central data acquisition system (CDAS). All tests were conducted at room temperature with appropriate fixtures (i.e., three-point bending fixture for HMA SCB and Marshall fixture for CMA mixtures).



### 3.4. Sample Fabrication

#### *3.4.1. Asphalt Concrete Mixtures*

##### Hot Mix Asphalt

HMA mixtures that were previously transported to the UNL testing lab in sealed buckets were taken out of containers and heated to 290°F, which is the recommended compacting temperature of the SPR mix. The mixture was left at this temperature for a minimum of two hours with occasional stirring of the mixture (e.g., every 30 minutes) to ensure uniform heating. After the two hours, HMA mixture was placed in a typical mixer, and cornhusk fibers were slowly added. Since the workability tended to decrease dramatically during mixing, the mixture was placed back in the oven every five minutes until the mixing of fibers was complete. The fiber-reinforced asphalt concrete (FRAC) mixture was subsequently placed in the oven for 30 minutes to allow temperature equilibrium after mixing. FRAC was then compacted using a standard gyratory compactor into a cylindrical tall sample of 150 mm in diameter and 170mm in height (Figure 8(a)). The tall samples were then cut into slices of 50 mm in thickness (Figure 8(b)), which were then cut into halves, and a notch of 15mm in length and a width of 2 mm was inserted in the middle (Figure 8(c)) to conduct SCB testing. By this method, a total of six SCB specimens were fabricated from one tall sample for each case, and their test results were averaged.

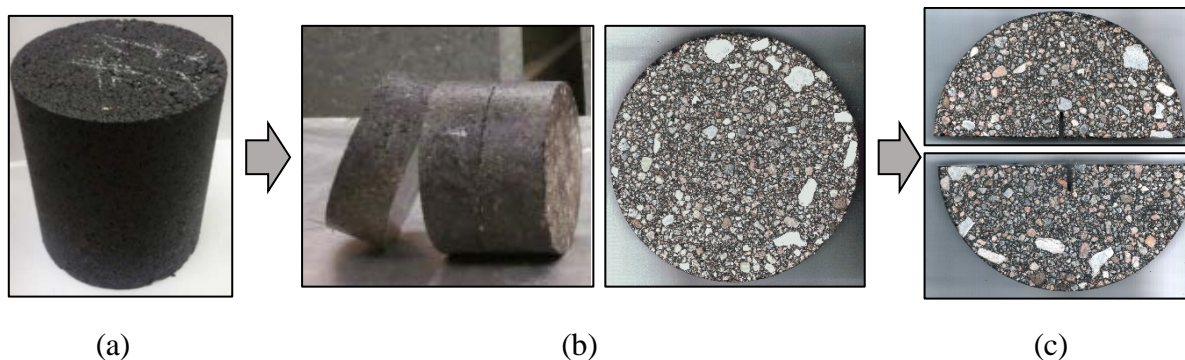


Figure 8: Fabrication of SCB specimen: (a) after compaction, (b) slicing and (c) notching.

### Cold Mix Asphalt

Cold mixes used in here were supplied by NDOT from distributing production plants around Nebraska. Similar to HMA, each mixture was transported in sealed containers to avoid evaporation of any light molecules. Due to the nature of cold mix and to use the Marshall testing fixture, the Marshall compactor (Figure 9(a)) was used to compact samples (Figure 9(b)) according to ASTM D6926-16. Fiber mixing in cold mix was also done by the similar mixer used in the HMA case. A total of three replicates as mandated by the Marshall test (ASTM-D6927–15) were compacted for each case by applying 50 blows on each side of the specimen.

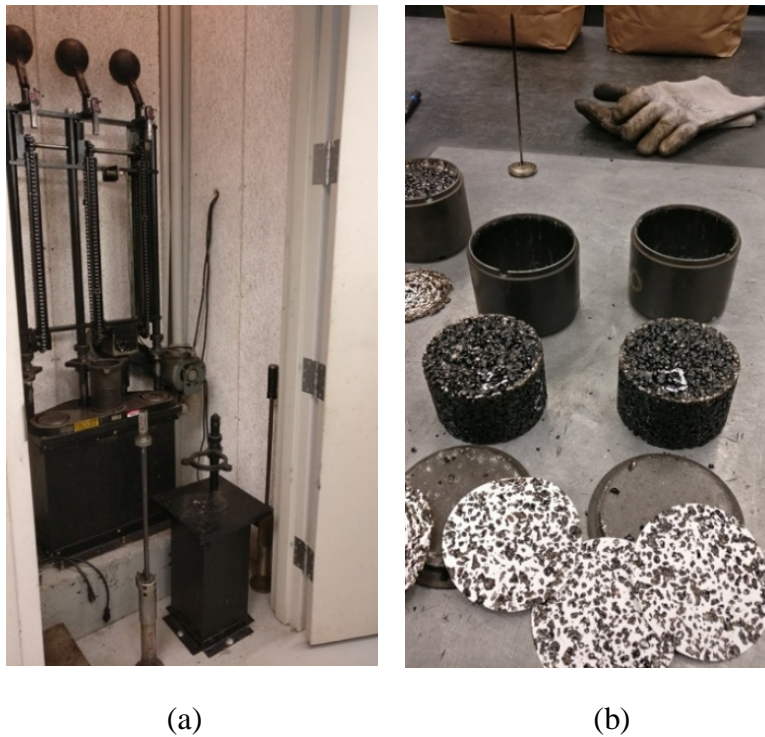


Figure 9: Sample fabrication for Marshall testing: (a) compactor, (b) samples after compaction.

For a workability test of the cold mix, the Cold Patch Slump Test (CPST) was adopted from a previous study (Chatterjee et al. 2005). The main set-up components were a standard Marshall hammer, wood containing unit, standard 4 in. x 8 in. PVC tube, and spreading tool (e.g., spatula). Cold mixture was put in the PVC container in two layers, each compacted by 5 blows of the Marshall hammer. Then the PVC container with the sample inside was temperature conditioned

to 1.7°C (35°F) to simulate winter temperatures at which cold mixes are usually laid. Figure 10 shows the CPST set-up.

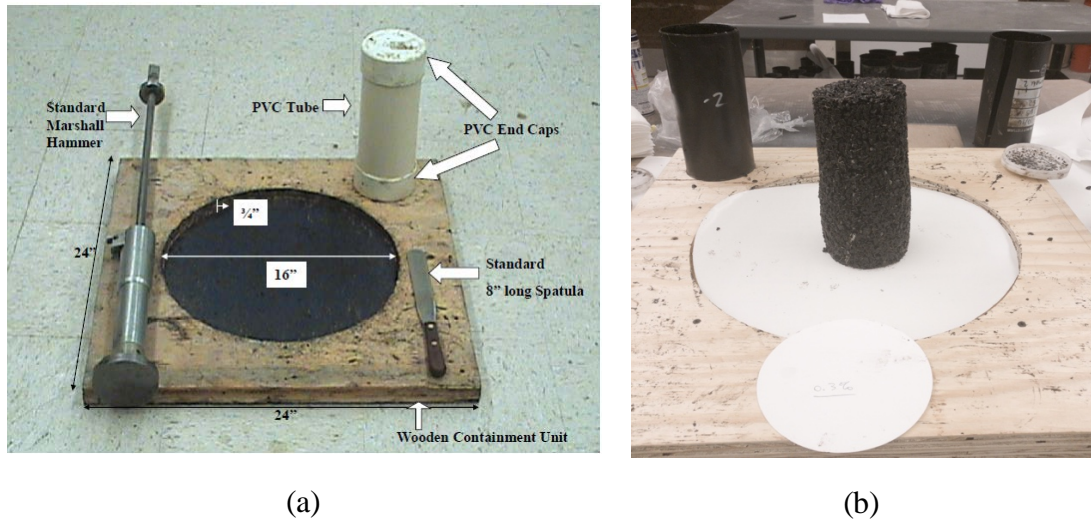


Figure 10: Cold patch slump test for workability test set-up: (a) by Chatterjee, Smit et al. (2005) (b) used in here.

Due to high workability of the cold mix, the samples would almost immediately fail without curing them after compaction. The curing serves to increase viscosity by reducing lighter molecules (oils) of the mixture so as to facilitate sample fabrication for laboratory testing. To investigate the proper curing method, loose cold mixture was placed in the oven at 140 °F, similar to the previous study (Chatterjee et al., 2006), and recorded the weight change with time. The elevated temperature accelerated the evaporation of light molecules. Two curing methods: loose mix curing and compacted mix curing were investigated. The results showed that loose mix curing is more effective: after approximately  $72 \pm 24$  hours the weight change saturated as presented in Figure 11.

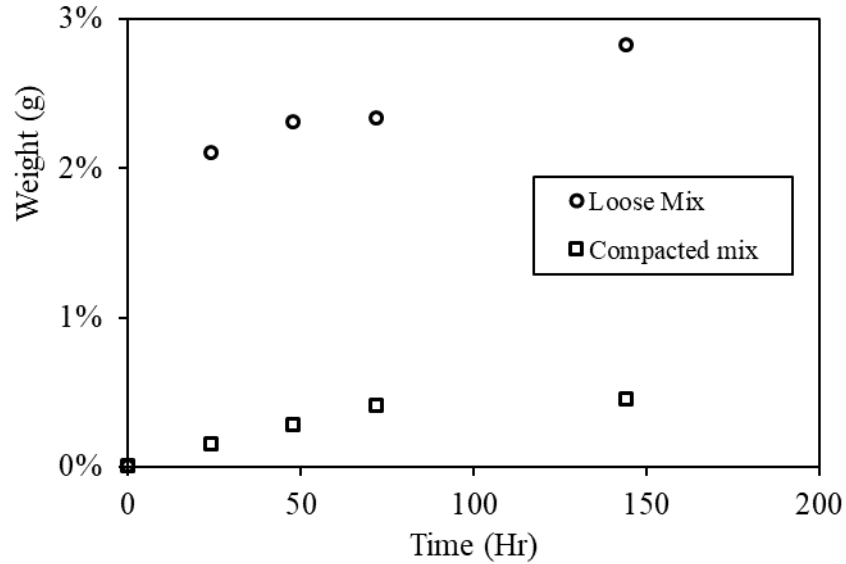


Figure 11: Weight loss of cold mix asphalt at 140°F.

### 3.4.2. Asphalt Binder Samples

#### Carbon Nano-modified Binder

Sample fabrication is the most important and critical task of this investigation. Since the scope of this study is to understand the influence of the carbon nano-fillers on the rheological properties of the binder, it is essential that these fillers are well dispersed. Nano-modification of the binder samples must meet two important criteria at the sample preparation stage:

1. Proper and uniform dispersion of the nano-filler within the binder; and
2. Retain the nano-level structure of the filler within the binder without aggregating.

The level of dispersion strongly depends on the type of filler used and the properties of the binder. Researchers have investigated the sample preparation process and it was observed that nano-particles with a high active surface area tend to aggregate at high mixing temperature.

In the preliminary investigation, two methods of mixing were tried. In the first trial, one of the samples were prepared using the high shear mixer. In the other method, the samples were prepared by manually mixing after adding the nanoparticles to the binder. In the first method, the nanomaterials were mixed to the binder using a Silverson High Shear Mixer. Approximately 500 grams of the binder was heated and then poured into an aluminum container. The container was then placed in a heater, and the mixing spindle was slowly lowered into the container, as shown in

Figure 12(b). The system was allowed to reach a thermal equilibrium, and the temperature was set to  $145 \pm 5$  °C. The speed of the mixer spindle was slowly raised from 200 rpm to 2,000 rpm. Nanoparticles were then slowly added into the binder within a time span of 15 to 20 min, and the sample was mixed for a period of 45 min. In the manual mixing method, the binder samples were taken into small containers of 20 oz capacity. Then, about 25 grams of binder was added to the containers and placed on a heater at  $145 \pm 5$  °C. Next, the appropriate amount of nano-filler was slowly added while mixing with a spatula.

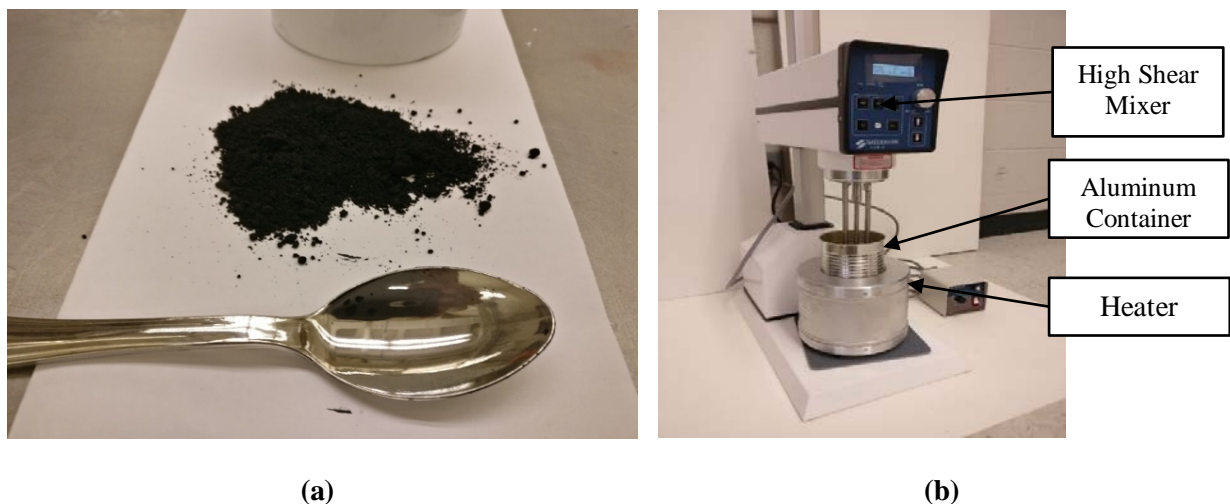


Figure 12: Nano-filler and mixing method: (a) nanostructured graphite-250 that was used in the preliminary investigation, (b) Silverson high shear mixer with the aluminum container and heater.

In the preliminary investigation, it was observed that both methods described above produced similar mechanical properties when the dosage of the nano-filler was less than 10 percent by the weight of the binder. The difficulty occurred with the high shear mixer when mixing at higher dosages of nano-filler more than 10 percent, and even more difficult in the case of polymer modified binders. The range of dosage for mixing with the high shear mixer could vary from filler to filler and hence such preliminary investigations were necessary. Due to the difficulty observed from the high shear mixer, all subsequent sample preparations for adding nano-filler or limestone filler to the binder were thus prepared by manual mixing.

## Chapter 4 Test Results and Discussions

In this chapter, test results are presented, and relevant discussions are given in detail.

### 4.1. Cornhusk Fibers

Typical stress-strain behavior resulting from tensile testing of cornhusk fibers is shown in Figure 13. It demonstrates the process of stretching a cornhusk fiber. Gradual increase of the load before the tensile strain of 5 percent indicated that the cornhusk fibers are not very stiff. A peak load at around 100 gf which corresponds to 16-17 percent of stain was observed.

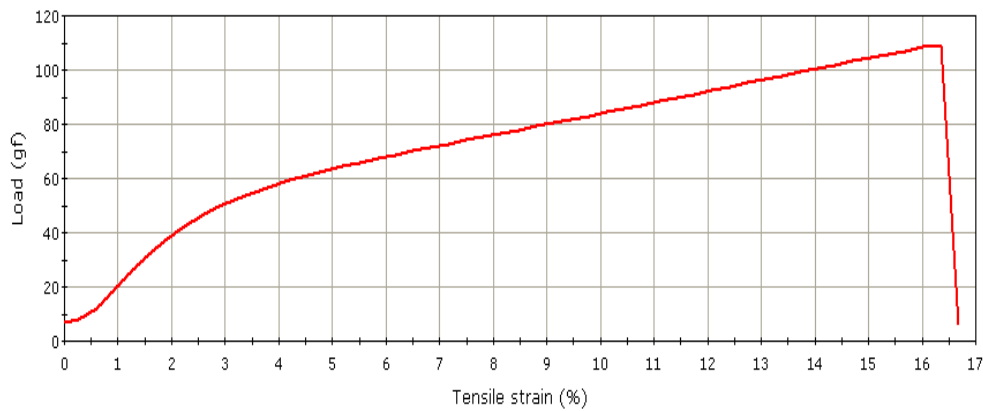


Figure 13: A typical stress-strain curve of cornhusk fiber.

Since preparation of asphalt concrete mixtures usually uses temperatures as high as 160 °C for 30 minutes, it is critical to determine the change of the mechanical properties of cornhusk fibers during this process. The obtained fibers were thus heated in an oven for 30 minutes at 55, 85, 115, 145 and 165 °C, respectively, and then the tensile testing of single fibers was conducted.

Figure 14 illustrates the effects of temperature of thermal treatment on tensile properties, including tenacity, elongation at break, Young's modulus, and energy (work of rupture) of cornhusk fibers. The tensile properties of fibers did not vary significantly as the temperature increased from 25 °C to 165 °C. The highest temperature of 165 °C was similar to the processing temperature of asphalt. Since cellulose degrades at a temperature higher than 230 °C, the temperatures of treatments could not affect the main component of cornhusk fibers significantly. The hemicellulose and lignin remaining in the fibers might be slightly affected by thermal

treatments at relatively high temperatures. However, the large variation of tensile strength values rendered the difference not significant.

Figure 15 demonstrates change in tensile characteristics such as tenacity, elongation at break, Young's modulus, and energy (work of rupture), of cornhusk fibers as thermal treatment prolonged. Overall, all the four tensile characteristics decreased slightly with the increased thermal treatments, which might degrade some non-cellulosic compositions that remained after fiber extraction from cornhusks. However, with the large variations, it can be implied that the difference among treatments at different time periods might not be statistically significant.

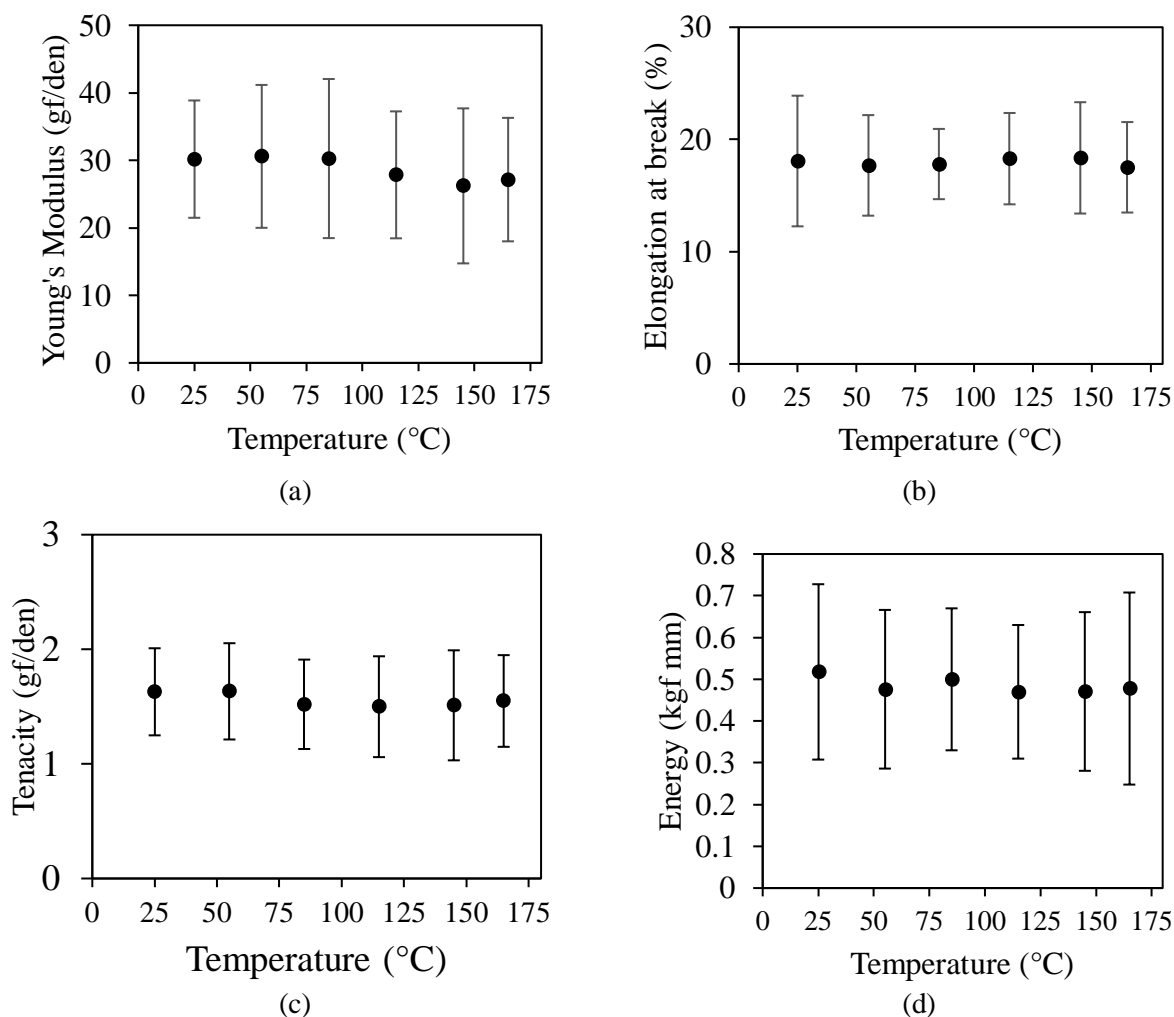


Figure 14: Mechanical properties of untreated fibers after 30 minutes exposure at different temperatures.

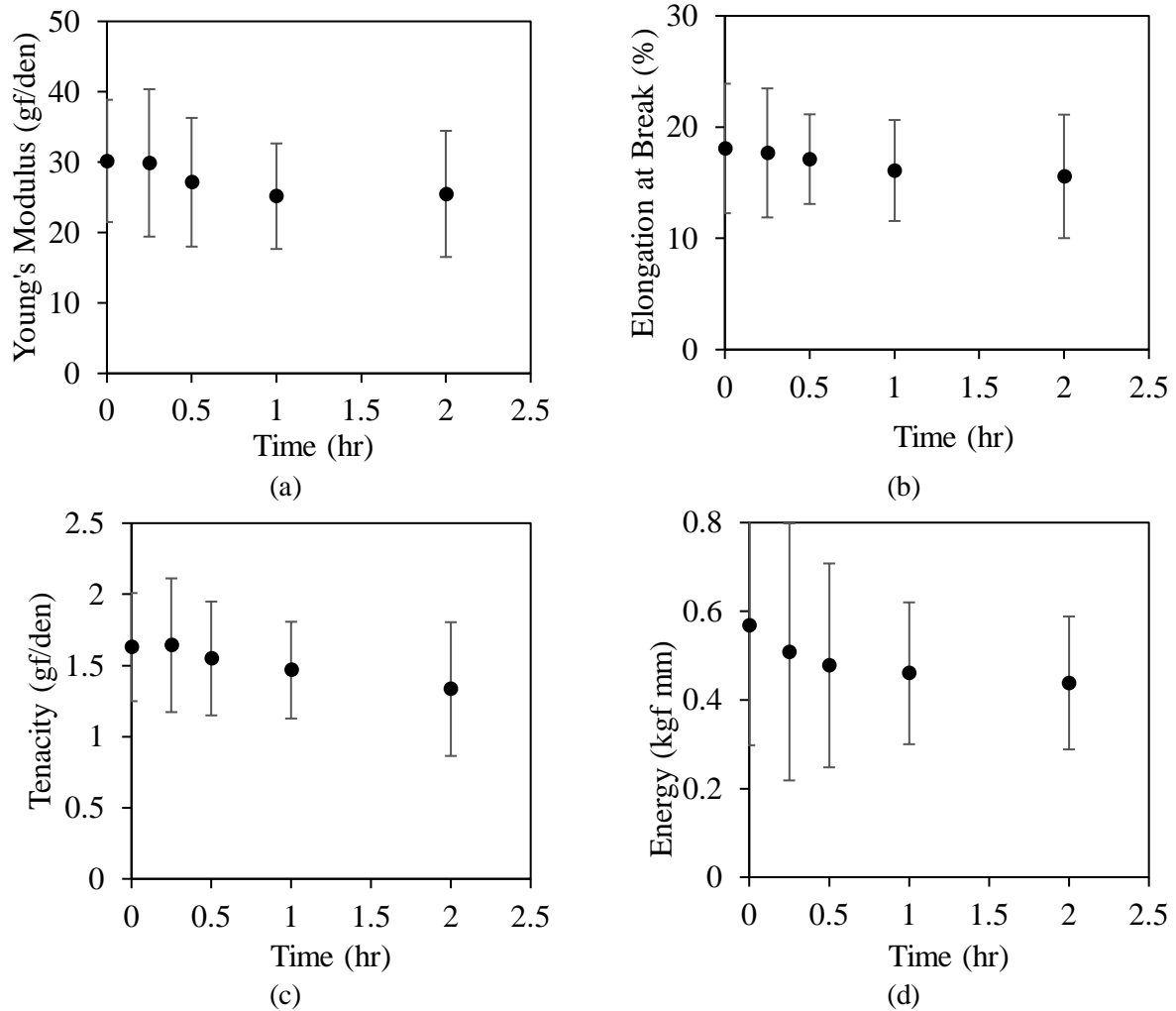


Figure 15: Influence of time spent at high temperature (160°C) on tensile properties of fibers.

#### 4.2. SCB Test Results of HMA with Cornhusk Fibers

Figure 16 show SCB test results of HMA mixtures. 10 mm fibers were added in the mixtures with fibers in two different percentages, 0.1 and 0.2 by the total weight. For a comparison purpose, a control case without fiber was also tested. For each case, four replicates were tested. In general, replicates showed a similar force-displacement behavior, thus average of replicates was obtained and plotted in Figure 16(d). As shown, with 0.1 percent of fibers, mixture stiffness and strength increased compared to the case without fiber, while those two mechanical characteristics were diminished with more addition of fibers (i.e., 0.2 percent addition).



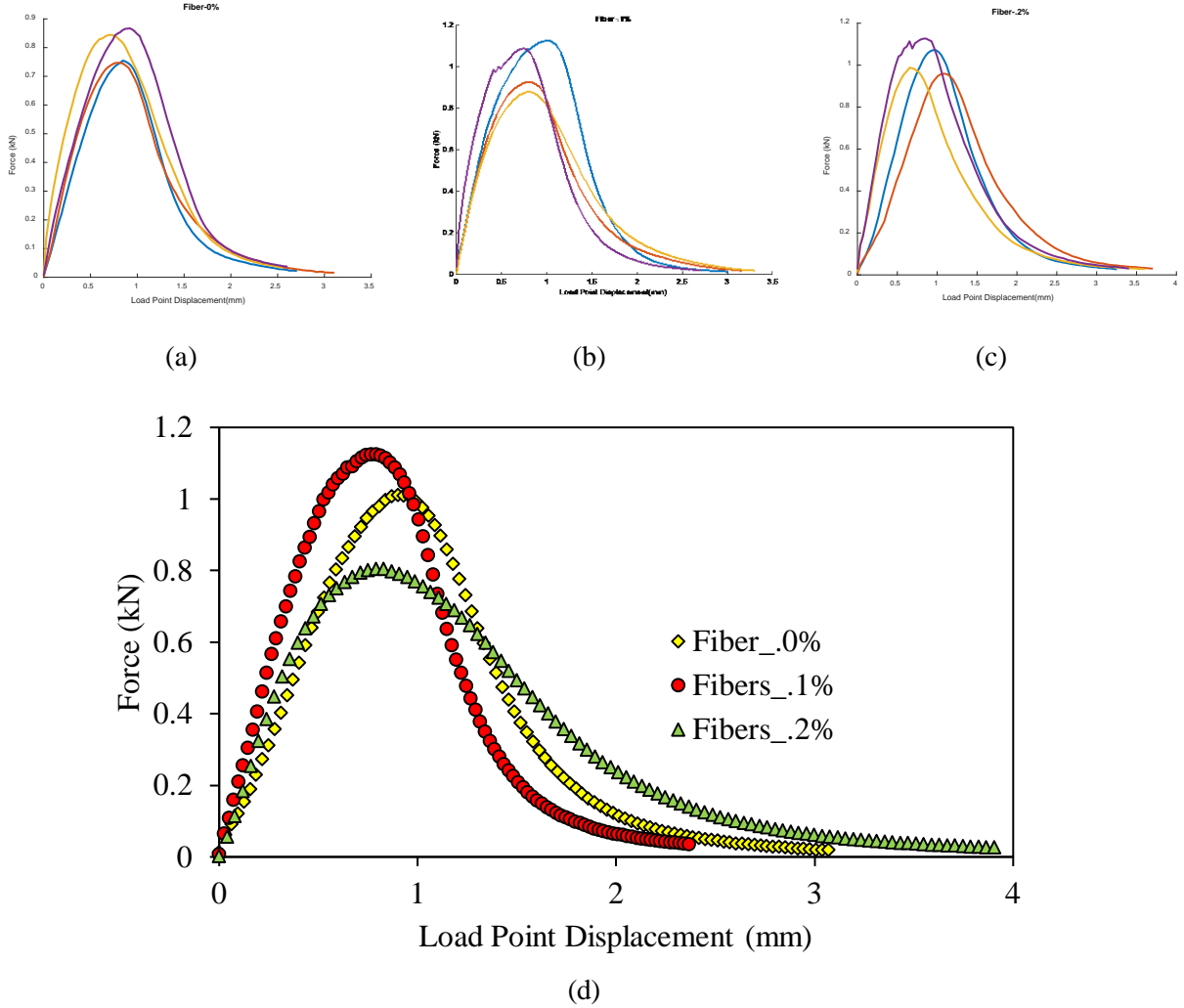


Figure 16: SCB test results at different content of 10-mm fiber: (a) control mixture, (b) 0.1 percent fiber content, (c) 0.2 percent fiber content, and (d) average of replicates.

In order to evaluate the effects of different fiber lengths, 20 mm long fibers were attempted, and test results are presented in Figure 17. Similar to the previous set, four replicates were tested for each case (i.e., control case and two other cases with different amounts of fibers: 0.1 percent and 0.2 percent). To compare the three cases in a simple manner, average force-displacement of replicates was obtained and plotted in Figure 17(d).

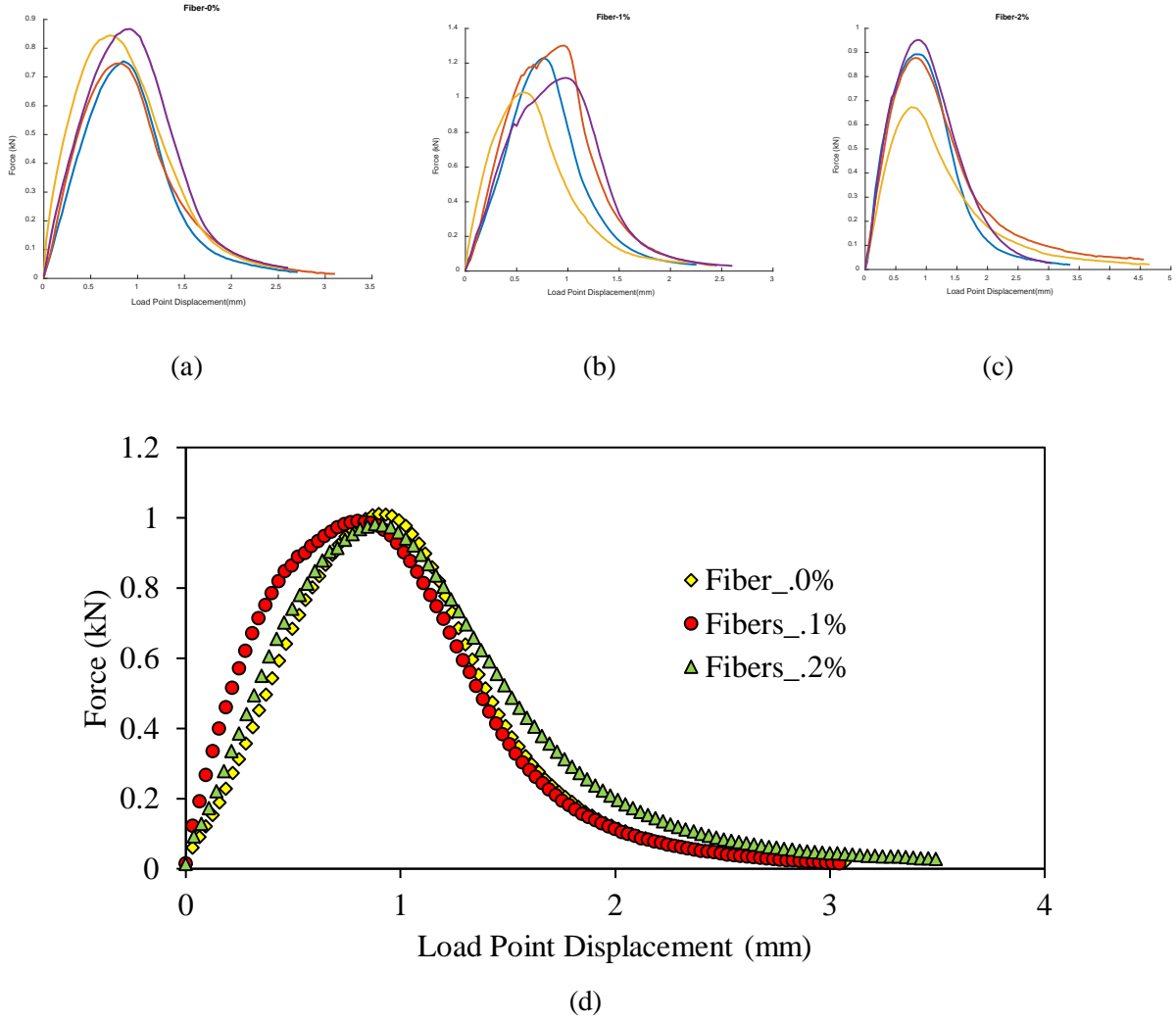


Figure 17: SCB test results at different content of 20-mm fiber: (a) control mixture, (b) 0.1 percent fiber content, (c) 0.2 percent fiber content, and (d) average of replicates.

As shown in Figure 17, with 0.1 percent of 20 mm fibers, mixture stiffness slightly increased compared to the case without fiber, while stiffness reduced back when 0.2 percent of fibers were added. In terms of strength, all three cases showed a similar behavior. Although further investigation is needed to make any definite conclusions, the insignificant (or even diminished) contribution of fiber addition on mechanical properties of asphalt concrete mixtures is attributed to an increase in fiber coagulation. In fact, at 0.2 percent fiber content, the fiber clogging was significantly high as demonstrated in Figure 18. Fiber clogging rendered mixing more difficult and

thus less attractive from practicality point of view. Uniform distribution of fibers is considered essential towards uniform and more reliable performance of asphalt concrete mixtures in field.

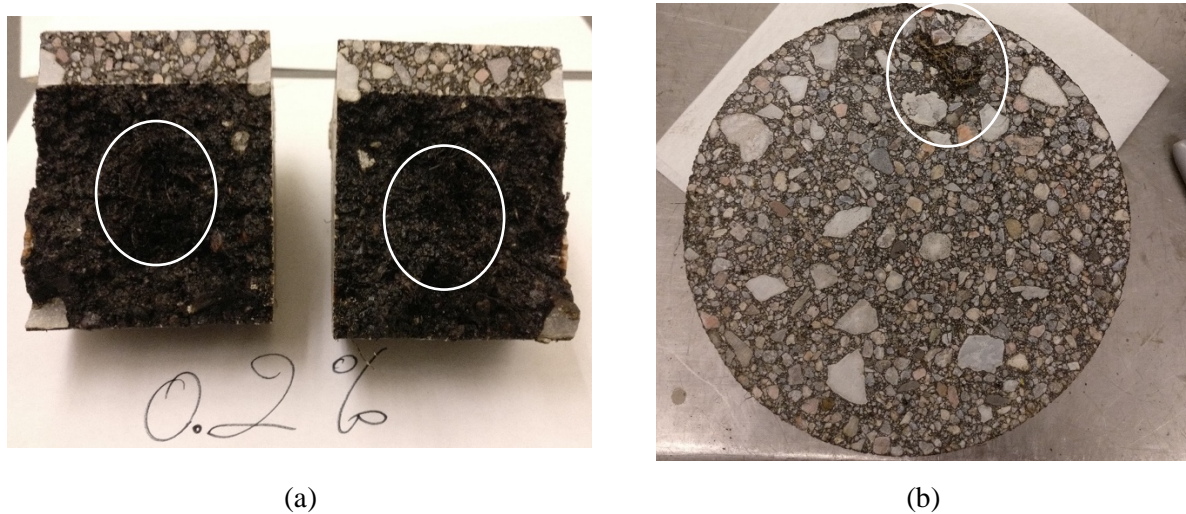


Figure 18: 20 mm fiber clogging at 0.2 percent fiber content.

#### 4.3. SCB Test Results of HMA with Synthetic Fibers

To gain a deeper understanding of the performance of natural fibers, cornhusk fibers were compared to a commercial synthetic fiber. The synthetic fiber chosen in this study is named ACE Fiber™ and made of aramid fibers and Sasobit wax. The aramid fibers are the reinforcing agents while the wax holds the otherwise light fibers together and facilitate mixing and fiber preparation. When mixing ACE Fiber™ to HMA at high temperatures, the wax is supposed to melt and allow the aramid fibers to disperse in the mixture.

The synthetic fiber mixing in the laboratory was conducted following the recommendation of the manufacturer. The fiber content was 0.05 percent by the weight of the mixture, and the fiber length was 45 mm as shown in Figure 19 (b). To compare the synthetic fibers to natural fibers, AC mixture samples with 45-mm long cornhusk fibers were also manufactured by putting 0.05 percent by the weight of the mixture (see Figure 19(a)). The same mixing method previously mentioned was used. Figure 19 (c) and Figure 19 (d) show the clogging issue observed during mixing when the 45-mm fibers were used. This observation is similar to the situation when higher fiber content (such as 0.2 percent) was attempted. To investigate whether the laboratory mixer was a factor

contributing to the clogging, two different laboratory mixers, one located at UNL's Civil Engineering Materials laboratory and the other located at the Nebraska Department of Transportation (NDOT), were used. The two mixers were different in terms of shape and mixer speed. The mixer located at UNL was cylindrically shaped, while the one at NDOT was shaped like a bowl and could mix at a higher speed. In each case, the FRAC mixture composition remained identical. After mixing, visually, the fiber clogging persisted regardless of the mixer used, and was still visible even after compaction (see Figure 19 (e)).

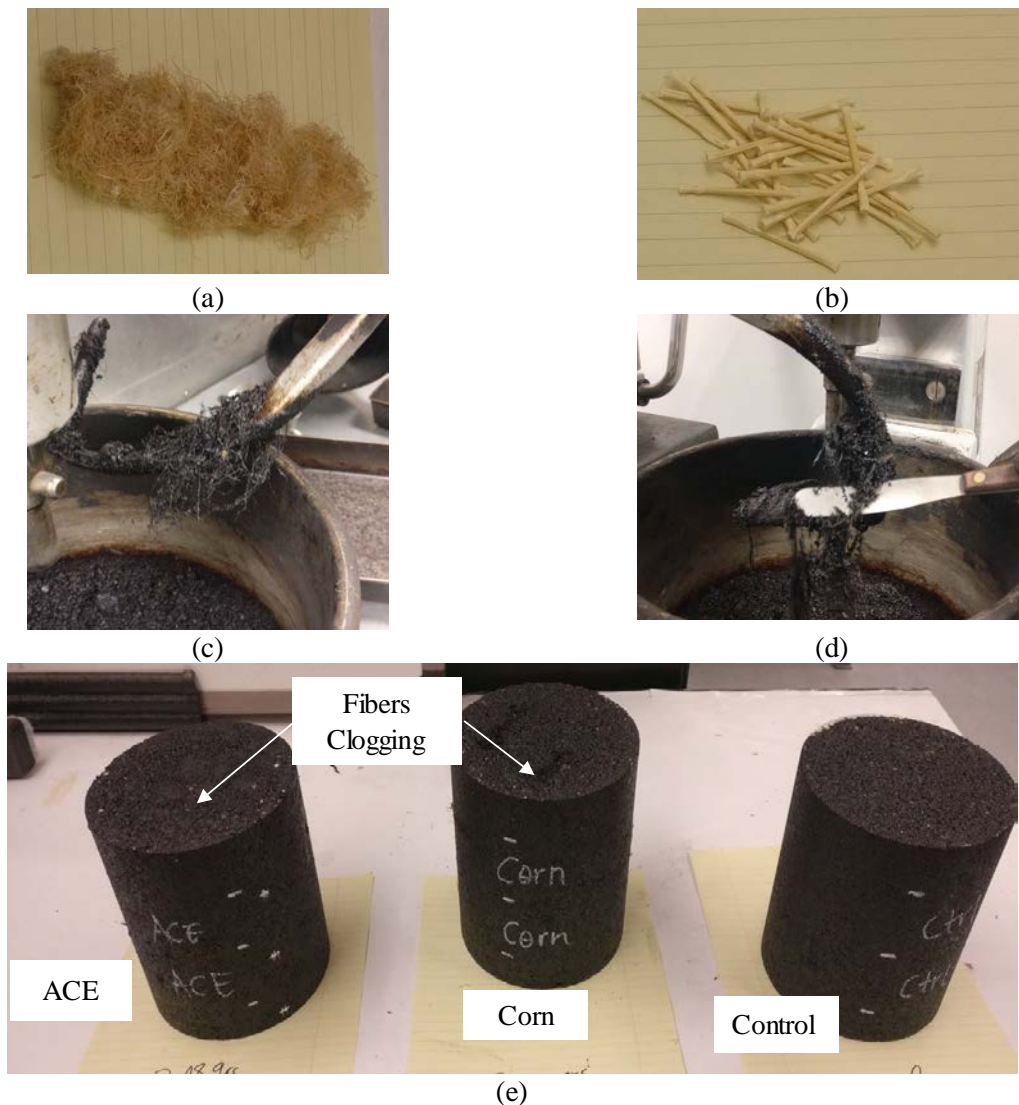
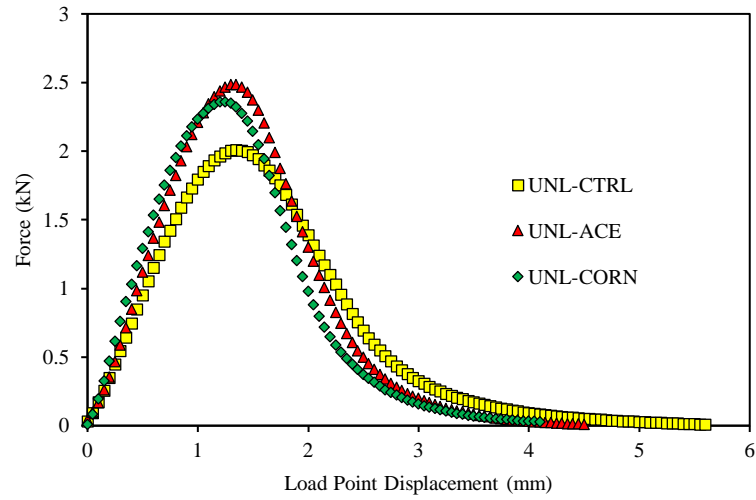


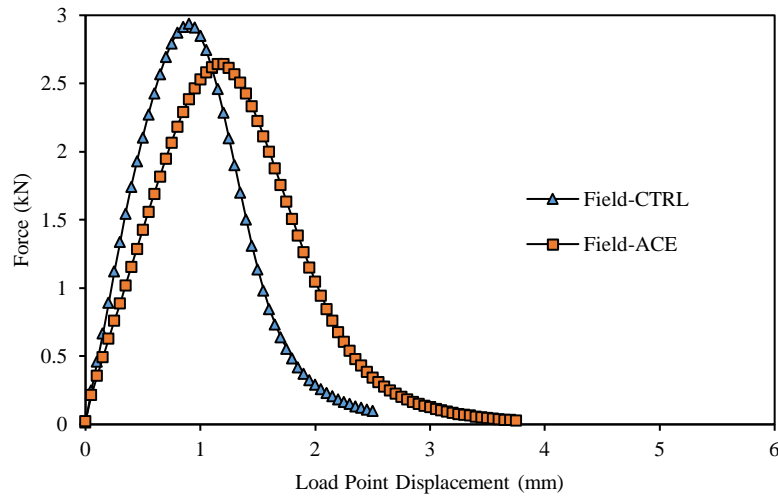
Figure 19: Comparison between natural and synthetic fibers during sample fabrication: (a) cornhusk fibers, (b) ACE Fiber™, (c) mixing of cornhusk fibers, (d) mixing of ACE Fiber™, and (e) compacted tall samples. Note: all fibers shown in this figure were 45-mm in length.

Clearly, achieving a uniform distribution of fibers using a typical laboratory mixer was not trivial. To obtain a better perspective of the actual field condition, synthetic (i.e., ACE Fiber™) FRAC and control samples from an asphalt production plant were obtained and compared by conducting the SCB test. The fibers used in FRAC from the plant were identical to those used in the laboratory-prepared FRAC mixtures. The FRAC from the plant were received, compacted, and sealed in a container to prevent aging. After visual inspection, samples with fibers did not exhibit any clogging issue at the surface. In fact, fibers remained imperceptible even after SCB testing. This suggests that a more uniform fiber distribution could be achieved at the plant.

Figure 20 shows SCB test results comparing synthetic fibers to natural fibers. In Figure 20(a), FRAC samples with either cornhusk fibers or ACE Fiber™ prepared at the UNL laboratory showed slightly higher stiffness and peak force compared to control. Figure 20(b) shows test results comparing two mixtures: plant-produced mixture without any fiber (i.e., control) and plant-produced mixture with ACE Fiber™. It appears that the addition of synthetic fibers might increase the displacement at failure and soften the mixture by reducing the stiffness, while it could reduce stiffness and strength of the mixture, although further testing and investigation is necessary to make any definite conclusions.



(a)



(b)

Figure 20: Load vs. displacement test results of 45-mm long fibers mixed and compacted at different locations: (a) UNL laboratory and (b) prepared at an asphalt production plant.

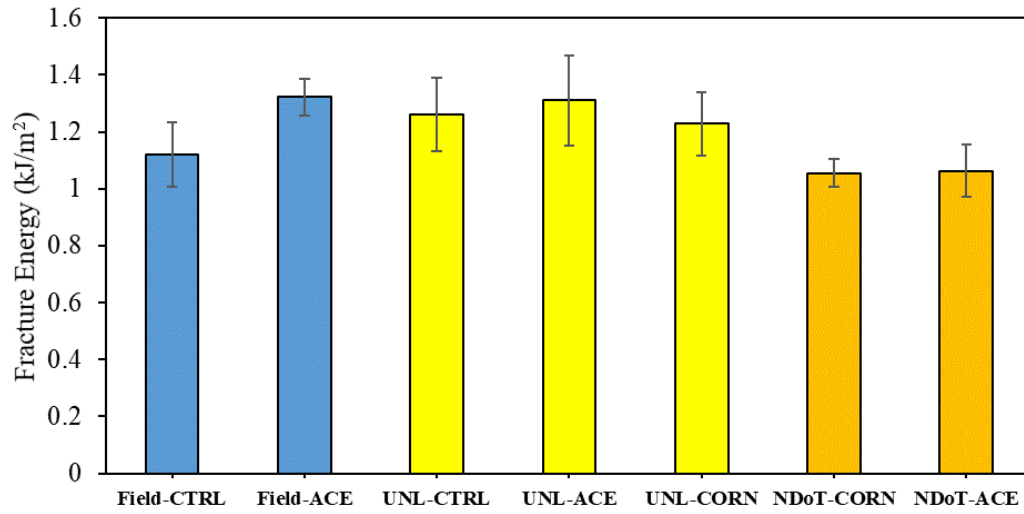
#### 4.4. Comparison Between Fibers

Further insights can be gained by calculating fracture-related parameters such as the fracture energy and flexibility index from the load-displacement curves shown in Figure 20. Fracture energy can quantify the amount of work done to fracture the specimen normalized to the fracture

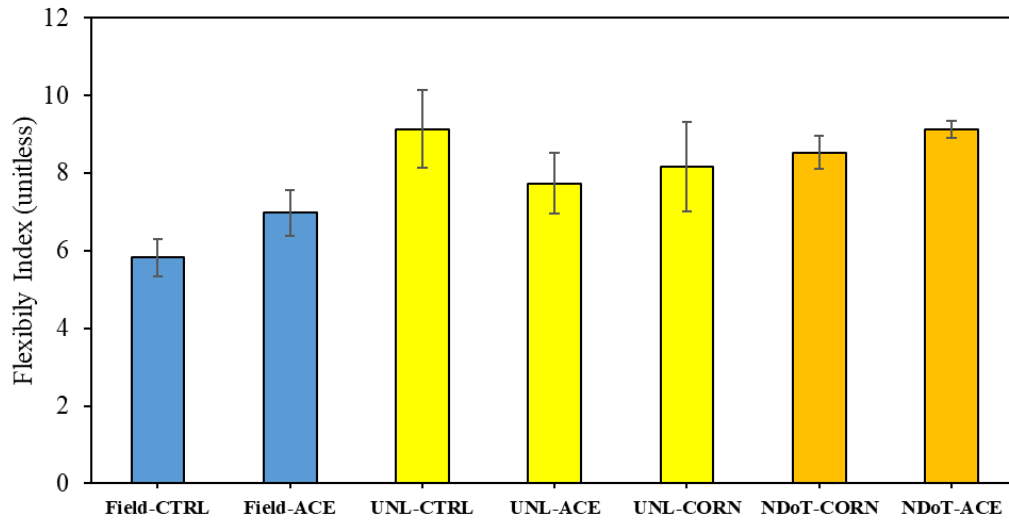
ligament. A previous study (Nsengiyumva 2015)) has shown that fracture energy could detect differences between AC mixtures. Another parameter, the flexibility index (FI) has recently been developed by researchers at the University of Illinois – Urbana Champaign (Ozer et al. 2016). FI is a useful indicator in that it takes into consideration the rate at which new fracture surfaces are being created by considering the post peak slope at inflection point. Furthermore, FI has shown a good correlation to the mixture performance in the field. It is noteworthy that higher FI is desired as it means that the fractured surface in the material happened at a slower pace.

Figure 21(a) shows fracture energy resulting from the all SCB tests for both mixture preparations. It can be noted that in Figure 21, control mixtures were different between plant and laboratory produced FRAC mixtures. It follows that due to the better distribution of fibers, FRAC produced from the plant experienced improvement in fracture energy compared to the control. The effect of the better fiber distribution is again manifested in higher repeatability (shown as error bars in the figure) of the plant FRAC results compared to the control HMA. It should be noted that, for the plant-produced mixture testing, a total of 12 SCB specimens were tested for each case and were averaged while for the laboratory mixtures the aforementioned four replicates per case were used.

Figure 21(a) implies that for the two mixtures prepared in the respective laboratories, irrespective of the type of fiber, there were lack of significant improvements in fracture energy from the addition of fibers. This could be attributed to the mediocre fiber distribution in the FRAC mixtures produced in laboratories. It can also be noted that cornhusk fibers performed similarly to the ACE Fiber™ in both laboratories.



(a)



(b)

Figure 21: Calculated fracture parameters from test results with standard deviation as error bars:  
(a) fracture energy, (b) flexibility index.



The FI results shown in Figure 21(b), similar to fracture energy, suggest that the FRAC mixtures produced from laboratory do not improve fracture resistance compared to the control case. However, for field (plant) mixtures, FI was improved by adding the synthetic fiber, once again confirming that uniform fiber distribution is critical in FRAC fracture performance.

#### 4.5. CMA Test Results

After testing HMA samples with different fibers, the possibility of incorporating fibers in cold mix was explored. Since cold mixes are usually used in winter, and typically by shoveling from container trucks, it was of great importance to first investigate the effect of fibers on workability. This is because workability is an essential criterion when choosing cold mix used in the field.

##### 4.5.1. Workability Test

In this study, workability test was conducted by varying fiber contents with the most problematic fiber geometry (i.e., 20 mm long fiber) since it would represent the difficulty in the field due to fiber clogging in the mix, if that is the case. The results show that, while the slump height was similar in all cases, the time at which the slump achieved quasi-linearly increased from around 10 minutes for the control mixture to 24 minutes for the mixture with 0.3 percent fibers. These results indicate that, although the time to reach a certain slump height was different from case to case, the similar slump height may enable a longer time in patching with fiber reinforced cold mixes.

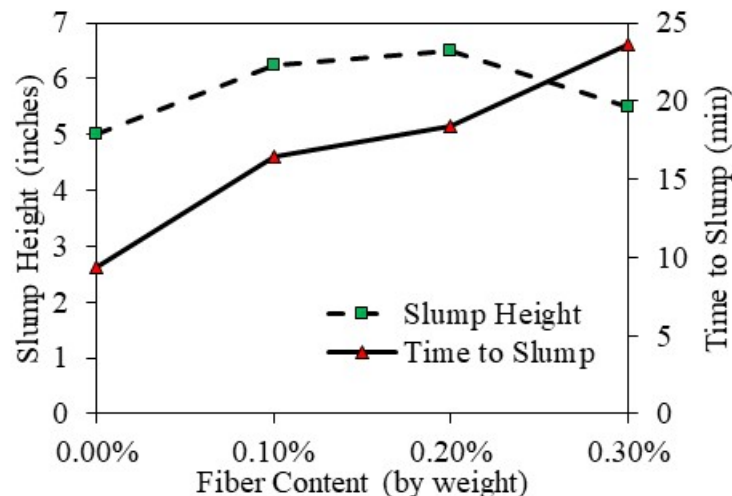


Figure 22: Results from workability test of 20 mm fibers at 0.3 percent content.

#### 4.5.2. Marshall Stability-Flow Test

Figure 23 shows a typical Marshall test result. From similar results obtained from different cases, the maximum force was taken to be the “Marshall stability”, and the displacement at which the maximum load was achieved was taken as “Marshall flow”.

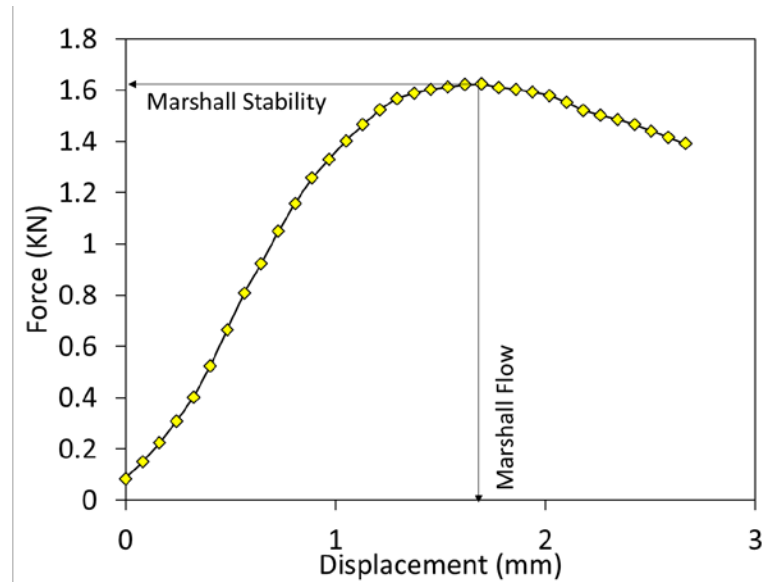
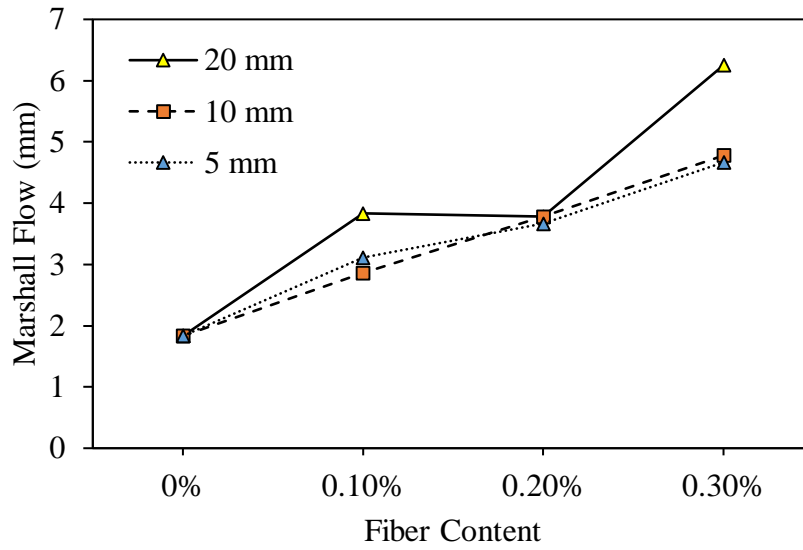
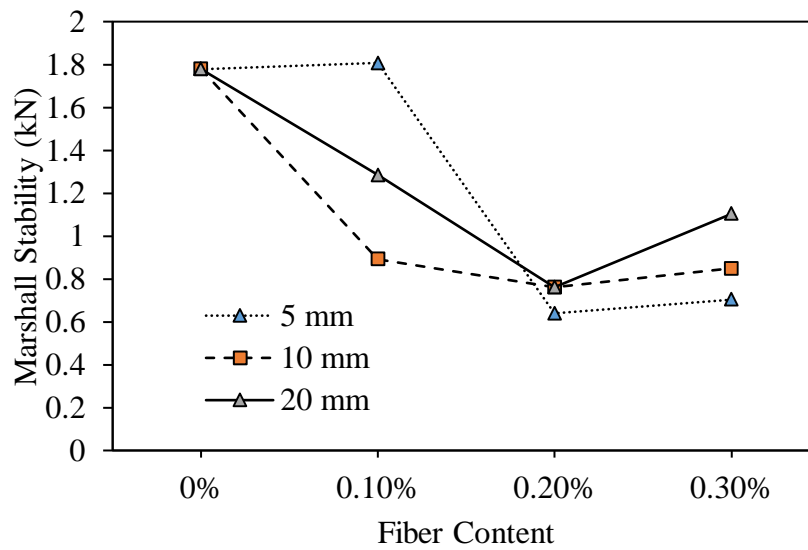


Figure 23: Typical Marshall test results showing force vs load point displacement (LPD).

Test results on the first cold mix (i.e., QPR) in terms of Marshall stability and Marshall flow are shown graphically in Figure 24. The results show that the flow increases (Figure 24(a)) with longer fibers and the trend was more dramatic when fiber contents increased. However, stability generally dropped with increasing fiber contents (Figure 24(b)).



(a)



(b)

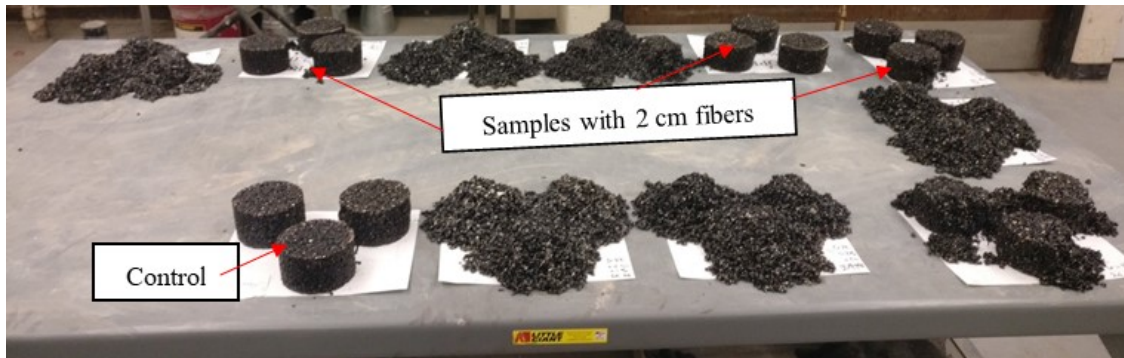
Figure 24: Test results of fiber reinforced cold mix: (a) Marshall flow, (b) Marshall stability.

One interesting observation from Figure 24(b) is that there is a trend of increasing stability at a longer fiber length. This observation was confirmed visually that samples with longer (e.g., 20 mm) fibers did not fall apart after testing regardless of the fiber content in contrast to shorter fibers (Figure 25(b)).

The second cold mix investigated was the Permapatch materials, which is more densely graded compare to QPR. The same testing matrix was attempted as in the QPR case. Adding fibers to Permapatch proved to be futile as all cases with fibers failed prematurely, and the mixtures failed shortly after compacting and even before testing (Figure 25(a)). It is hypothesized that the relatively dense gradation of Permapatch was not compatible with the addition of fibers since less space was available for fibers to be placed in the mix. It can also be hypothesized that the emulsified binder used in Permapatch is incompatible with cornhusk fibers due to some unconceived absorption issues.



(a)



(b)

Figure 25: Failure of cold mixes (a) Permapatch (material failed shortly after compaction and before testing), (b) QPR material 24 hours after testing showing coherent samples with long fibers.

## 4.6. Nano-filler Modified Asphalt Binder and Mastic

### *4.6.1. Preliminary Investigation*

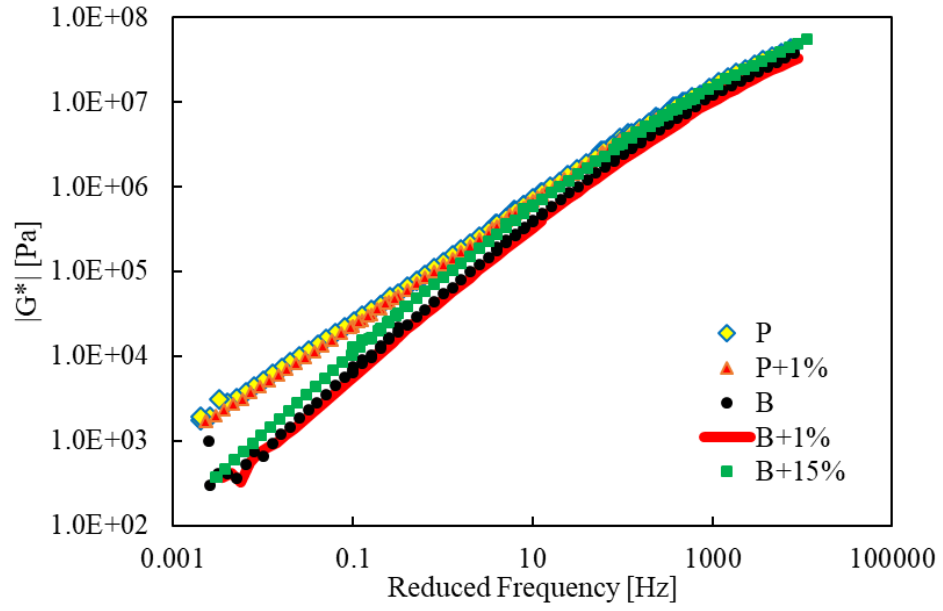
For preliminary investigation, the base binder and the polymer modified binder were added with a nano-filler, Nanostructured Graphite-250 (NG-250). Two dosages of 1.0 percent and 15 percent (by weight) for the base binder, and 1.0 percent (by weight) for the polymer modified binder were prepared. Subsequently, rheological investigation was carried out on the samples. Table 6 shows each sample, sample ID, and rheological tests conducted.

Table 6: Test Samples with Different Dosage and the Tests Conducted on These Samples as Part of the Preliminary Investigation

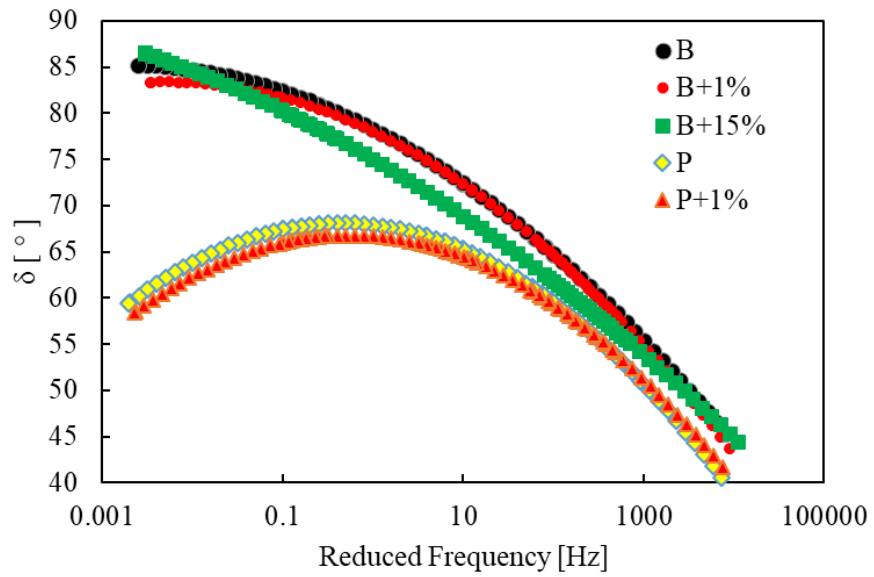
Sample	ID	Frequency Sweep	Amplitude Sweep	Temperature Sweep
PG 49-34	B	✓	✓	✓
PG 49-35 + NG-250 (1%)	B+1%	✓	✓	✓
PG 49-35 + NG-250 (15%)	B+15%	✓	–	–
PG 64-34	P	✓	✓	✓
PG 64-35 + NG-250 (1%)	P+1%	✓	✓	✓

### Frequency Sweep Test Results

For the binders presented in Table 6, frequency sweep tests were conducted at different temperatures of 0, 10, 25, and 45 °C, varying the frequency from 0.1 to 10Hz with a constant strain amplitude such that the behavior was well within the linear viscoelastic regime. The strain amplitude applied to the samples was 0.01 percent at all temperatures. Master curves of dynamic shear modulus ( $|G^*|$ ) and phase angle ( $\delta$ ) were obtained by shifting the data at different temperatures to a reference temperature of 25 °C using the time-temperature superposition principle. Figure 26 shows master curves of all five different binders. It can be observed that the dosage of 1.0 percent of NG-250 did not change the mechanical properties of the binders (both base binder B and polymer-modified binder P). A stiffening effect of NG-250 was observed when the base binder B (PG 49-34) was mixed with 15 percent of NG-250.



(a)



(b)

Figure 26: Master curve for base binders and its modified form formed by adding different dosage of NG-250 carbon filler to B and P (a)  $|G^*|$  values vs frequency (b)  $\delta$  values vs frequency.

### Amplitude Sweep Test Results

The binder samples presented in Table 6 were subjected to an amplitude sweep test where the strain amplitude was varied from 0.0001 percent to 100 percent at different temperatures and frequencies. The amplitude sweep was performed at 0 °C and 45 °C and at two different frequencies of 0.1 Hz and 10 Hz. Figure 27 shows amplitude sweep test results of the polymer-modified reference binder (P) and its nano-filler modified binder (P+1%). As shown, there was no considerable influence of carbon nano-filler NB-250 at a dosage of 1.0 percent.

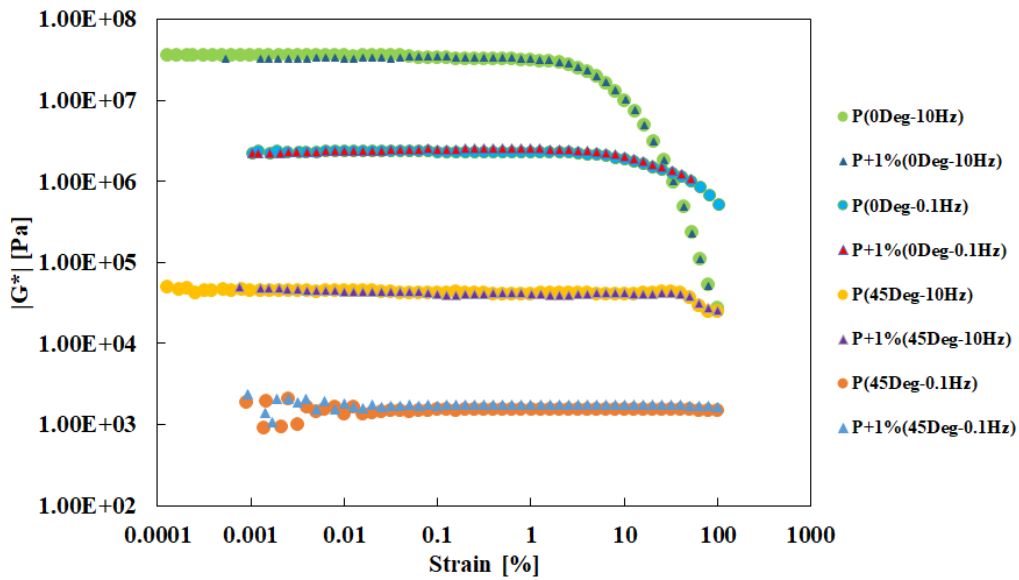
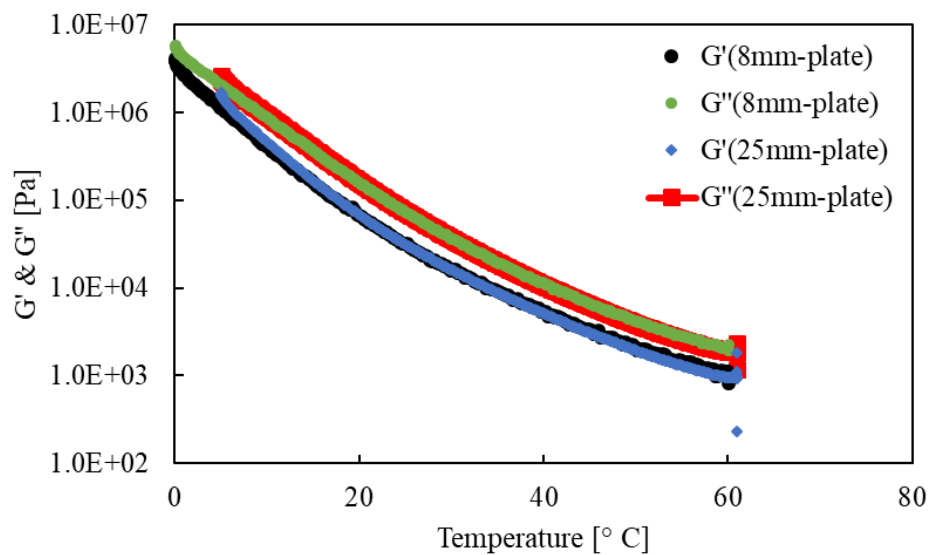


Figure 27: Strain sweep data at 0 °C and 40 °C at frequency 0.1 and 10 Hz for PG64-34 binder and its nanofiller modified binder at a dosage of 1.0 percent.

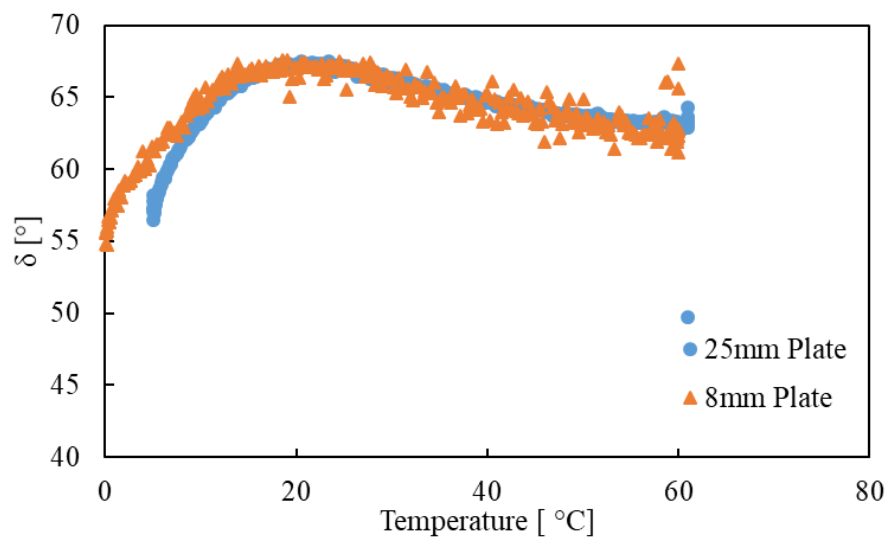
### Temperature Sweep Test Results

In the temperature sweep tests, the samples were subjected to a temperature ramp superimposed with an oscillatory loading of constant strain amplitude and frequency. The temperature was reduced at a constant rate of 5 °C/min from 60 °C to 0 °C, and the response of the sample was monitored. The sweep tests were carried on the base binder B with two test geometries of 8 mm and 25 mm diameter plates, and a gap of 0.5 mm was selected as shown in Figure 28. It was observed that both the geometries gave similar results showing the properties observed were independent of test geometry. This also indicates that the temperature ramp rate induced was not

fast enough to create a substantial temperature gradient across the binder sample. Moreover, the temperature sweep results were highly dependent on the frequency as shown in Figure 29.



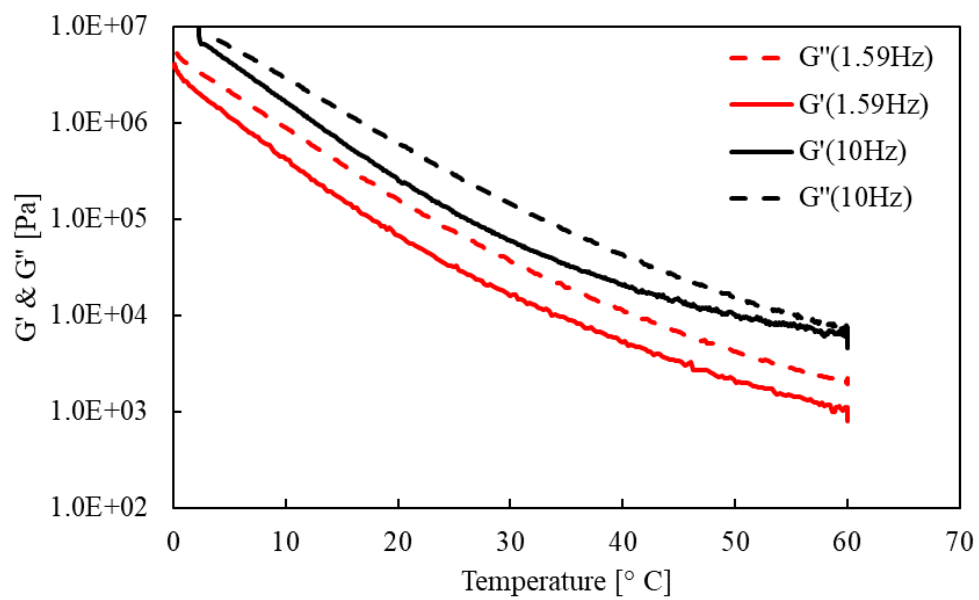
(a)



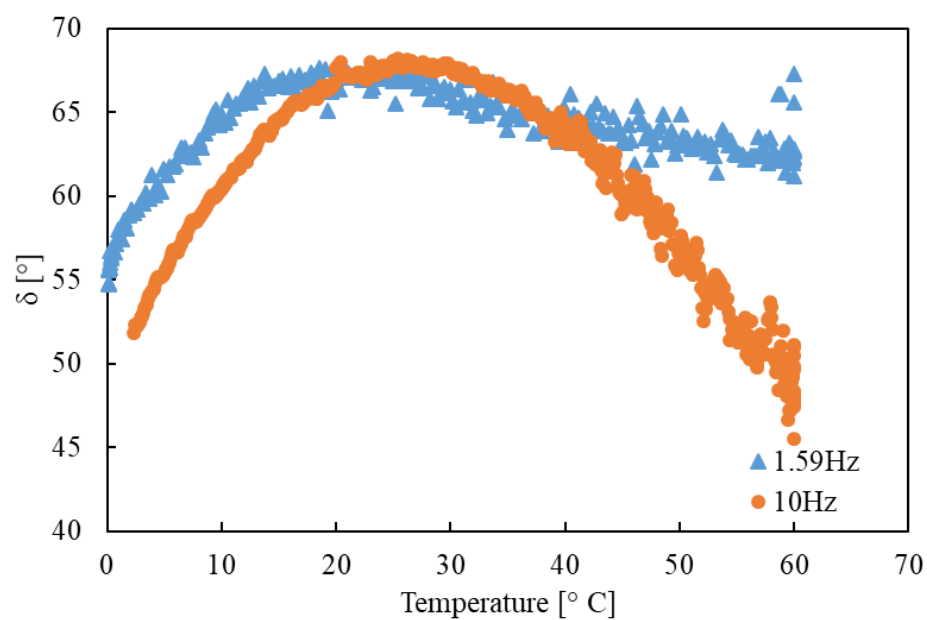
(b)

Figure 28: Temperature sweep: (a) storage and loss modulus, and (b) phase angle for 8 mm and 25 mm parallel plate of base binder.





(a)



(b)

Figure 29: Temperature sweep for base binder (a) storage and loss modulus (b) phase angle at different frequencies.

### Findings from the Preliminary Test Results

Based on the above preliminary investigation, the following conclusions were made.

- The linear viscoelastic properties of the binder did not change much with the graphite nanoparticle at small dosages.
- The dosage of the graphite nanoparticle around 1 percent to 5 percent by weight of the binder is considered low to introduce any thermomechanical changes in the parent binder.
- When heated to high temperatures, the graphite nanoparticles seem to settle at the bottom of the container, which causes somewhat non-uniform distribution of the particles.

#### *4.6.2. Primary Investigation*

For primary investigation, changes in the rheological properties at two different phases (i.e., the binder phase and the mastic phase) were attempted by introducing two distinct types of carbon nano-fillers. This primary investigation focused on the influence of adding carbon nano-fillers on the linear viscoelastic properties and performance-related characteristics such as fatigue resistance, rutting potential, and temperature susceptibility of the binder and mastic samples. The two carbon-based fillers used in this study are presented in Table 5.

One is an artificial graphite with a particle size less than 1  $\mu\text{m}$  and a surface area of 352  $\text{m}^2/\text{g}$ , whereas the other nano-filler is a carbon black which has a much smaller particle size at around 0.03  $\mu\text{m}$  with an active surface area of 254  $\text{m}^2/\text{g}$ . There are several factors that could influence the fillers' ability to interact with the binder. The active surface area and size of particles are key factors that could potentially influence the overall performance of the nano-modified binders. In addition, the ability of the nano-fillers to impart major changes to the performance of the binder lies in the nano-scale dispersion of the fillers and chemical interactions with the binder phase.

Notations used to represent the binder samples prepared by adding different fillers are presented in Table 7. For instance, notation "B" would represent the base binder (PG 49-34), which is an unmodified binder obtained from Flint Hills. To the base binder, a particular dosage of filler was added to obtain the nano-modified binders. For example, "B + F1(15%)" would mean that the base binder was modified by adding filler F1, which is 15 percent by the weight of the base binder.

Similarly, “P” would denote the polymer-modified binder (PG 64-34) obtained by adding 4 percent by the weight of SBS polymer to the base binder (B).

Table 7: Notations Used to Represent the Binder Samples Prepared in the Current Study

Notation	Description
B	Base Binder, PG 49-34
B + F1 (15%)	PG 49-34 + Filler F1 (15% by weight of binder)
B + F1 (25%)	PG 49-34 + Filler F1 (25% by weight of binder)
B + F2 (15%)	PG 49-34 + Filler F2 (15% by weight of binder)
B + F2 (25%)	PG 49-34 + Filler F2 (25% by weight of binder)
P	Polymer Modified Binder (B + 4% SBS Polymer), PG 64-34
P + F1 (10%)	PG 64-34 + Filler F1 (10 % by weight of binder)
P + F2 (10%)	PG 64-34 + Filler F2 (10 % by weight of binder)

The notations used to represent the mastic samples are presented in Table 8. Asphalt mastic is composed of binder and fillers (less than 75  $\mu\text{m}$  size particles), limestone filler was selected to make mastic samples. It is important to note that the notations used to describe the mastic samples are different compared to the ones used for the binder samples. In this study, the notation for mastic is based on the overall weight percentage of the asphalt concrete typically used in Nebraska. Usually the binder content within the asphalt concrete would be around 4 to 6 percent by the weight of the entire mixture, and in the current scenario it is assumed to be 5 percent by the weight of the mixture. The state of Nebraska recommends a dust to binder ratio (D/B), that is filler to binder ratio in the mixture, to be between 0.9 to 1.7. In this study, the D/B ratio is assumed to be 1.0, which implies that the mixture would contain limestone filler content of 5 percent (same as the binder content) by the weight of the mixture. Thus, the notation “B + LS” would mean a mastic prepared by mixing an equal proportion by the weight of the base binder (PG 49-34) and limestone filler because the D/B of 1.0 was assumed. The notation “B + LS (4.6%) + F1 (0.4%)” would mean

a mastic prepared by adding an equal proportion by the weight of the filler mixture (limestone + filler F1) and binder, where the limestone to filler (F1) ratio would then be 4.6 to 0.4. The abovementioned mastic samples were prepared to understand the influence of nano-filler in a more realistic sense that one could typically observe in the AC mixture by replacing parts of the filler with nano-sized particles.

Table 8: Notations Used to Describe the Mastic Samples Prepared in the Current Study

Notation	Description
B + LS	B (5% by weight of AC) + Limestone Filler (5% by weight of AC)
B + LS (4.6%) + F1 (0.4%)	B (5% by weight of AC) + Limestone Filler (4.6% by weight of AC) + Filler F1 (0.4% by weight of AC)
B + LS (4.0%) + F1 (1.0%)	B (5% by weight of AC) + Limestone Filler (4% by weight of AC) + Filler F1 (1% by weight of AC)
B + LS (4.6%) + F2 (0.4%)	B (5% by weight of AC) + Limestone Filler (4.6% by weight of AC) + Filler F2 (0.4% by weight of AC)
B + LS (4.0%) + F2 (1.0%)	B (5% by weight of AC) + Limestone Filler (4% by weight of AC) + Filler F2 (1% by weight of AC)
P + LS	P (5% by weight of AC) + Limestone Filler (5% by weight of AC)
P + LS (4.6%) + F1 (0.4%)	P (5% by weight of AC) + Limestone Filler (4.6% by weight of AC) + Filler F1 (0.4% by weight of AC)
P + LS (4.6%) + F2 (0.4%)	P (5% by weight of AC) + Limestone Filler (4.6% by weight of AC) + Filler F1 (0.4% by weight of AC)

#### Frequency Sweep Test Results

Frequency sweep tests were carried out on the samples shown in Table 7 and Table 8. The tests were carried out at 0, 10, 25, and 45 °C, and the frequency was varied from 0.1 Hz to 10Hz at each of the temperatures. The strain amplitude selected was 0.01 percent such that the response was

well within the linear viscoelastic limit. It can be observed that different nano-fillers influence the base binder differently, as shown in Figure 30. Nano-filler F1 showed an increase in the stiffness of the base binder at both dosages (15 percent and 25 percent), but when compared to nano-filler F2, the stiffening effects were not the same. Nano-filler F2 showed much more dramatic stiffening effects compared to F1 at the same dosage (i.e., 15 percent). This shows that stiffening effects are highly dependent on the filler types, and the way they interact with the binder phase can dictate the mechanical response of the blended material.

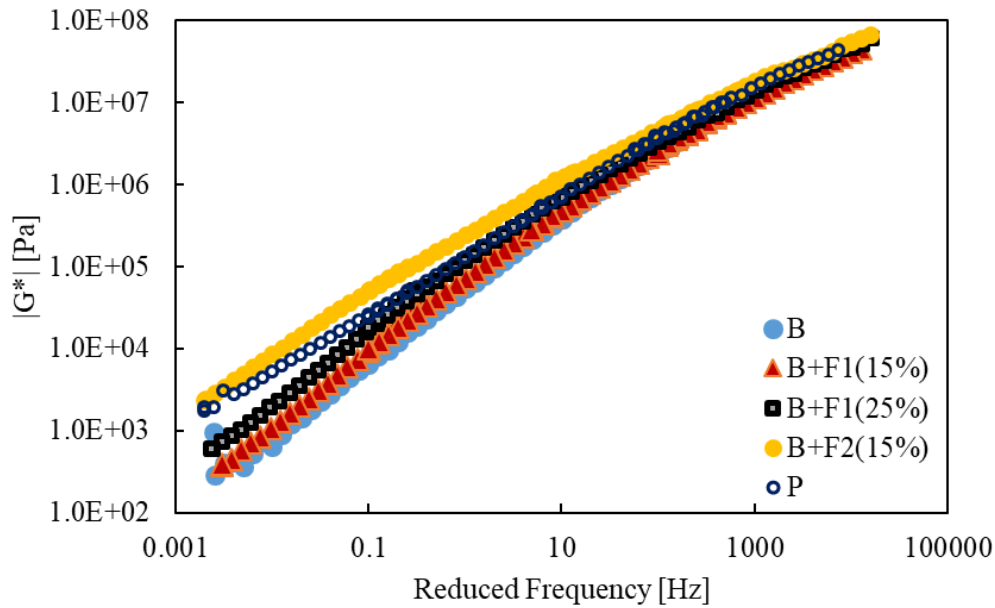


Figure 30: Master curves for base binder and its nano-modified binder using fillers F1 and F2 at a dosage of 15 percent and 25 percent; the polymer modified PG 64-34 is shown for comparison.

Similar investigation was carried out on the polymer modified binder (PG 64-34), as shown in Figure 31. It can be observed that the nano-filler F1 does not influence the mechanical properties of the polymer modified binder, whereas nano-filler F2 shows considerable stiffening effects. In order to investigate the influence of these nano-sized fillers in the presence of other mineral aggregate fillers, mastic samples (binder mixed with mineral fillers) were prepared by adding limestone filler to the base and polymer modified binder together with nano-filler F1 or F2. The

master curve plots of all samples tested are shown in Figure 32 and Figure 33. It was observed that the nano-filler F1 reduced the viscoelastic properties when the carbon filler was added to base binder, whereas F2 improved the properties only slightly. In case of polymer modified mastic, F1 did not change the viscoelastic properties, whereas F2 showed considerable improvements.

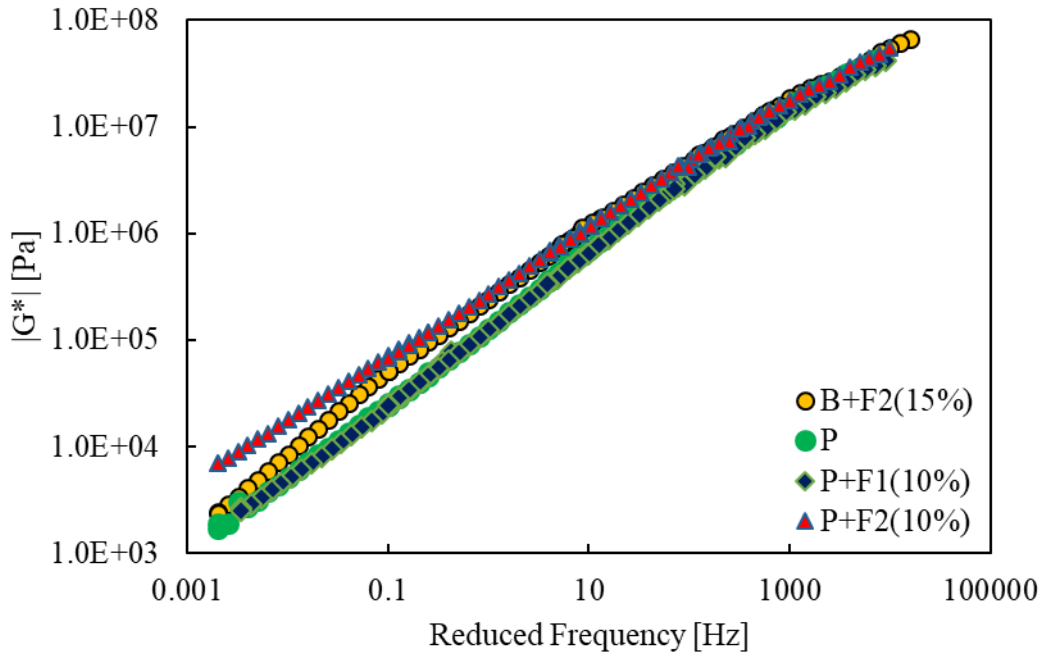


Figure 31: Master curve for polymer modified PG 64-34 and its corresponding nano-modified binder using nano-filler F1 or F2 at a dosage of 10 percent; also included is the base binder modified with nano-filler F2 (15percent).

In Figure 32, it can also be seen that the effects of nano-filler F1 on mechanical properties of the limestone mastic were trivial at both replacement dosages (0.4 percent and 1.0 percent) when compared to the base mastic (B + LS). However, nano-filler F2 showed slight stiffening of the base mastic, and the level of stiffening increased with more addition. In Figure 33, it can be observed that the nano-filler F1 does not influence the mechanical properties of the PG 64-34 mastic, whereas nano-filler F2 shows a stiffening effect over intermediate and high temperatures.

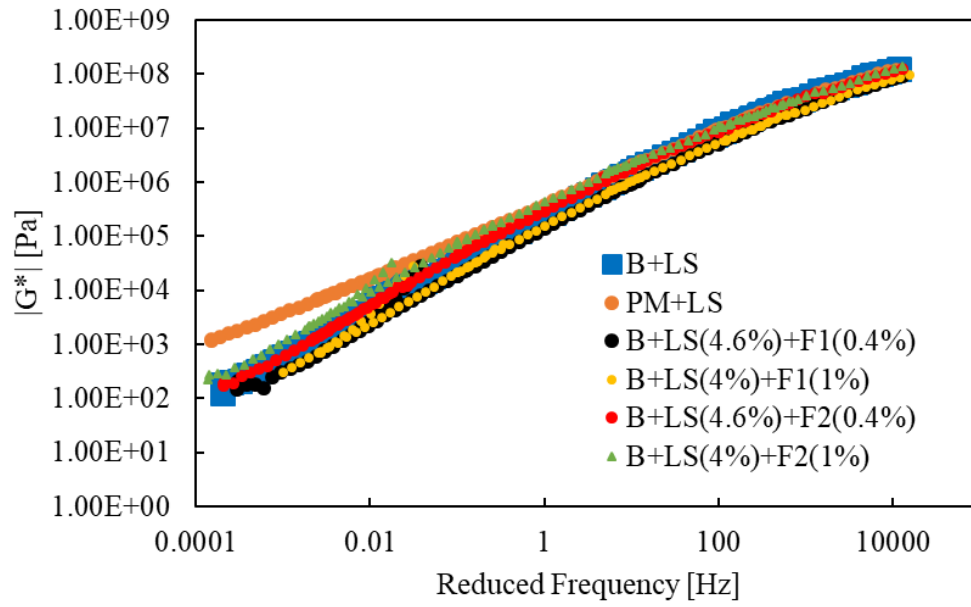


Figure 32: Mastic master curves for base binder modified by limestone filler and its corresponding nano-modified mastic samples.

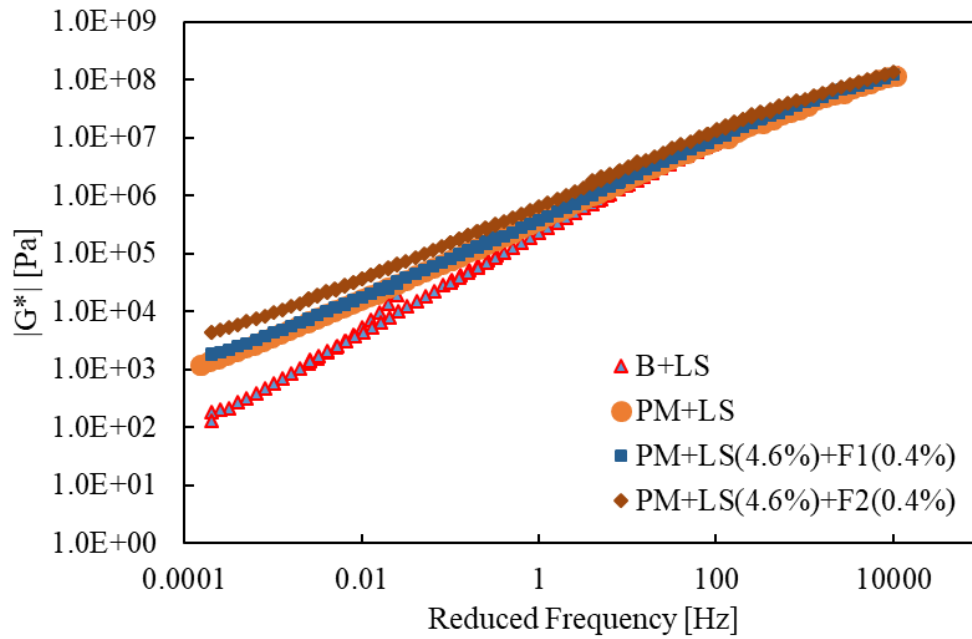
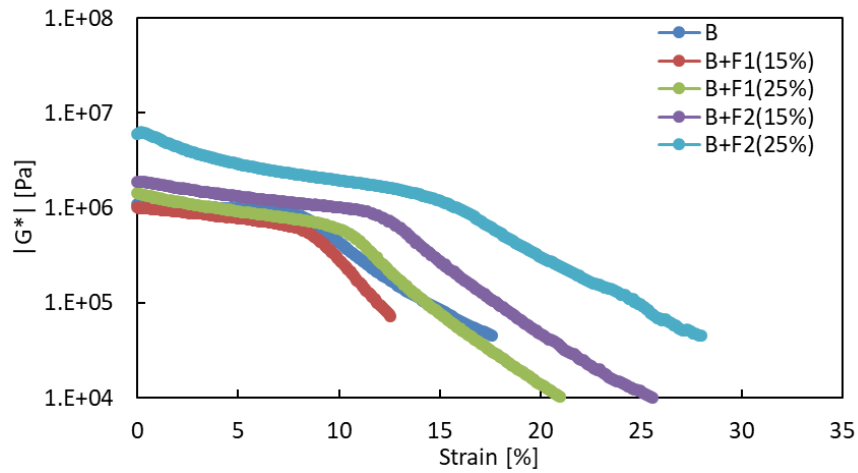


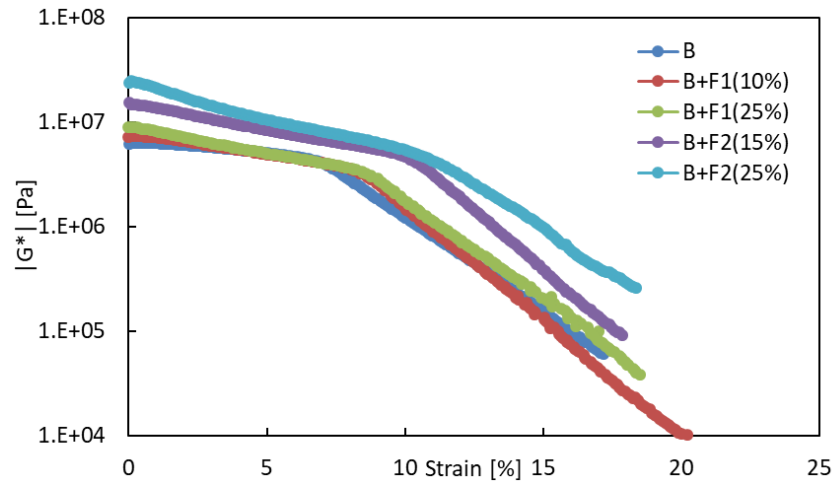
Figure 33: Mastic master curve plots for base binder mastic, polymer modified mastic, and its corresponding nano-modified mastics.

### Amplitude Sweep Test Results

The amplitude sweep tests were performed for the samples shown in Table 7 to assess material behavior under a whole range of strains from small (linear viscoelastic) to non-linear behavior and finally to damage. Toward that, the strain was increased linearly from 0.0001 percent to 100 percent at two different temperatures. Figure 34 shows the amplitude (in strain) sweep test results of the base binder (B) and its nano-modified binders (B + F1 or F2 in different addition rates) at 20 °C (Figure 34 (a)) and 10 °C (Figure 34 (b)), respectively.



(a)



(b)

Figure 34: Amplitude sweep results for base binder PG49-34 and its nanomodified binder by fillers F1 and F2 at (a) 20 °C (b) 10 °C.



Test results show the changes in the values of  $|G^*|$  (dynamic shear modulus that indicates material stiffness) as the strain amplitude increases. It can be observed in the graph that beyond a particular strain amplitude there is a much faster drop in the  $|G^*|$  values. This amplitude can be considered as a transition stage of strain at which considerable nonlinearity (or damage) has been initiated. It can be observed that both nano-fillers enhance the strain limit at both temperatures. Also, an increased resistance was observed with increasing dosage for both fillers. The influence of the nano-filler F2 was more than F1.

Figure 35 shows the strain sweep test results from the mastic samples (PG 64-34 binder mixed with limestone filler with or without nano-filler F1 or F2) at two different temperatures. Similar to previous test results, both nano-fillers enhanced the strain limit at both temperatures, while the enhancement was more obvious at 10 °C. Between the two nano-fillers, F2 showed much more resistance to increasing strains than F1.

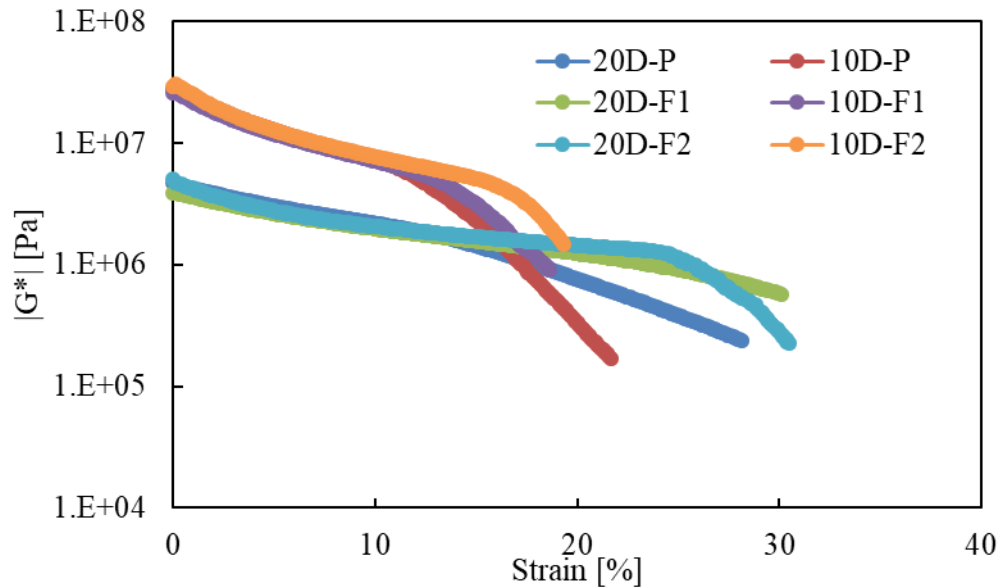


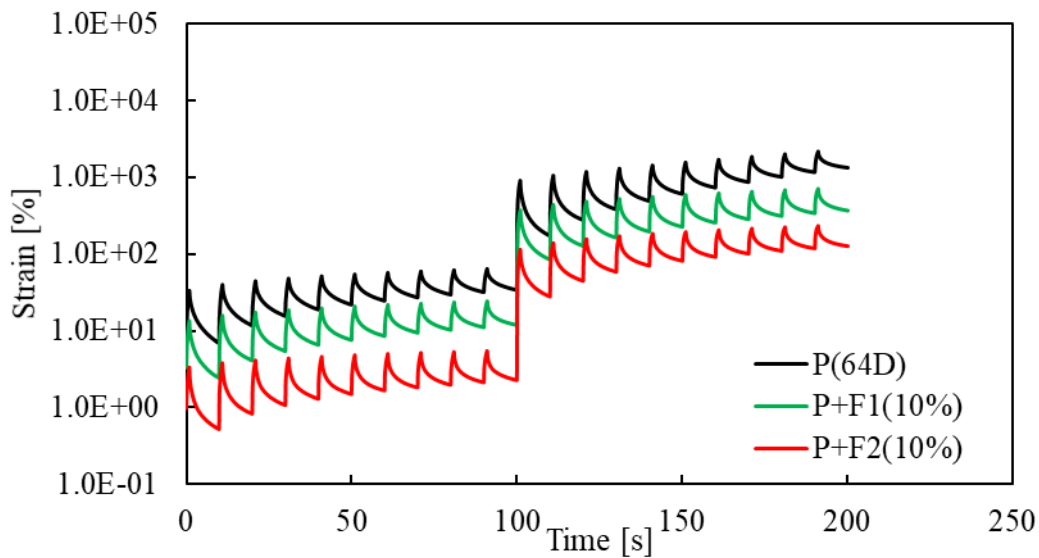
Figure 35: Amplitude sweep results for mastic samples for PG64-34+LS and its modified mastic obtained by replacing part LS by F1 and F2 at 20 °C & 10 °C.

#### Multiple Stress Creep and Recovery (MSCR) Test Results

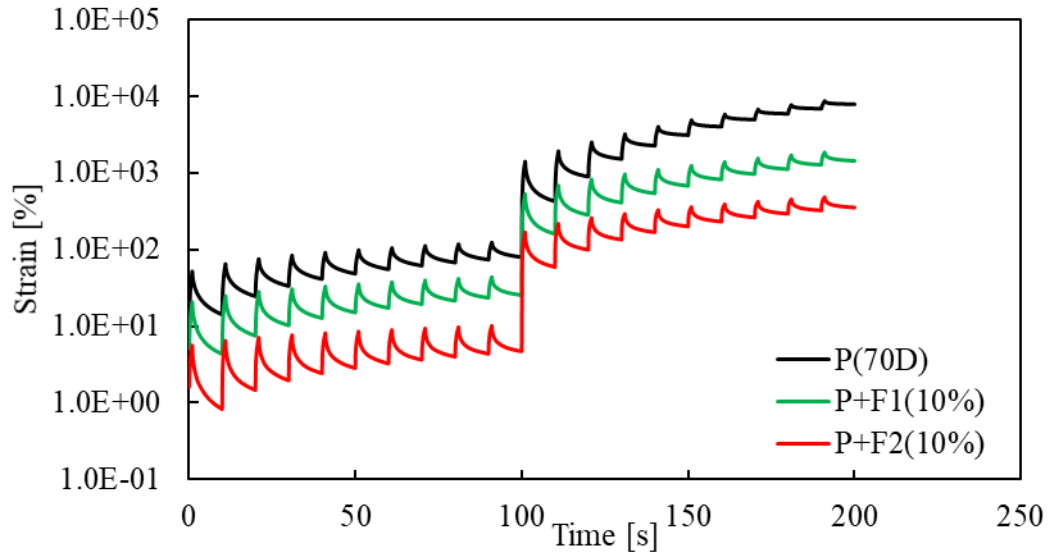
In order to evaluate the effects of nano-fillers on permanent deformation behavior of binder, multiple stress creep and recovery (MSCR) tests were performed on PG 64-34 binder and its nano-

filler modified binders and mastic samples at different temperatures. The MSCR tests are useful to assess the influence of the elevated surface temperatures of the pavement on the rutting susceptibility. During the MSCR tests each binder sample was subjected to cycles of creep and recovery such that 1-sec of creep time and 9-sec of recovery time was given. Ten cycles were applied at a creep stress of 0.1 kPa, followed by another 10 cycles at a creep stress of 3.2 kPa (AASHTO 2009). At the end of each cycle, the sample will have certain unrecoverable strain, which accumulates with each cycle. The larger the unrecoverable strain, the more likely the binder is susceptible to permanent deformation and hence more prone to rutting. Three temperatures (64, 70 and 76 °C) were selected to account for the influence of temperature.

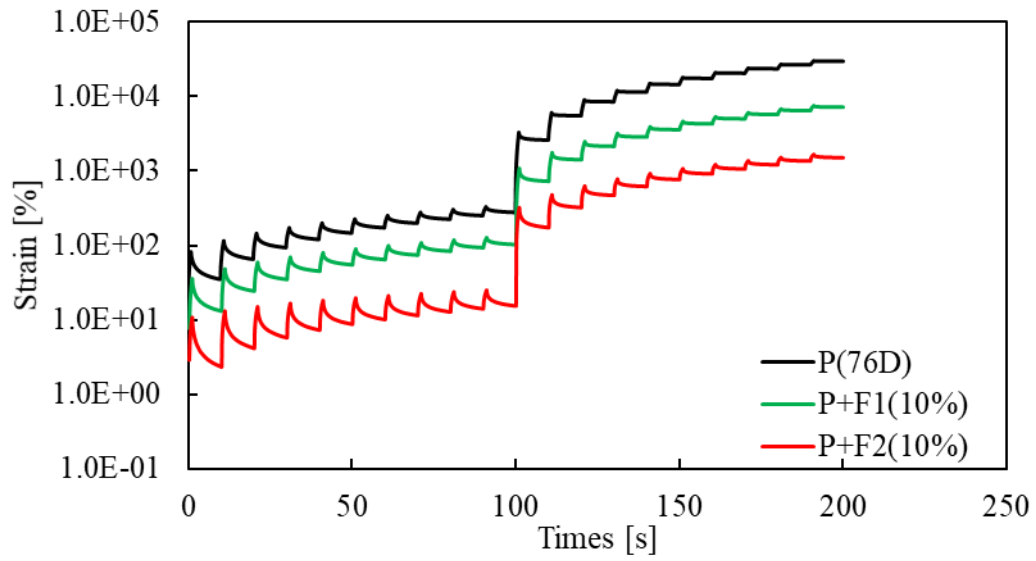
Figure 36 shows the results of the MSCR tests at different temperatures for the PG 64-34 binder and its modified binders using nano-fillers F1 and F2 at a dosage of 10 percent. It can be observed that the nano-fillers could improve the resistance to permanent deformation at all temperatures attempted. The filler F2 was more effective than F1.



(a)



(b)



(c)

Figure 36: MSCR test results for polymer modified binder and its nano-modified binders (a) 64°C, (b) 70°C, and (c) 76°C.

As observed in Figure 30, B + F2 (15%) showed improved linear viscoelastic properties in comparison to polymer modified binder P at intermediate and elevated temperatures up to 64 °C. In order to assess if the addition of filler F2 could provide similar improvements to the high temperature rutting susceptibility of the base binder, MSCR tests were performed at two temperatures (50 °C and 64 °C). Figure 37 shows the MSCR test results. As shown, base binder modified with nano-filler F2 is more susceptible to permanent deformation with weak recovery of strains at higher temperatures compared to polymer modified binder. This indicates that plastic deformation potential of binders could be different from linear viscoelastic properties at elevated temperatures.

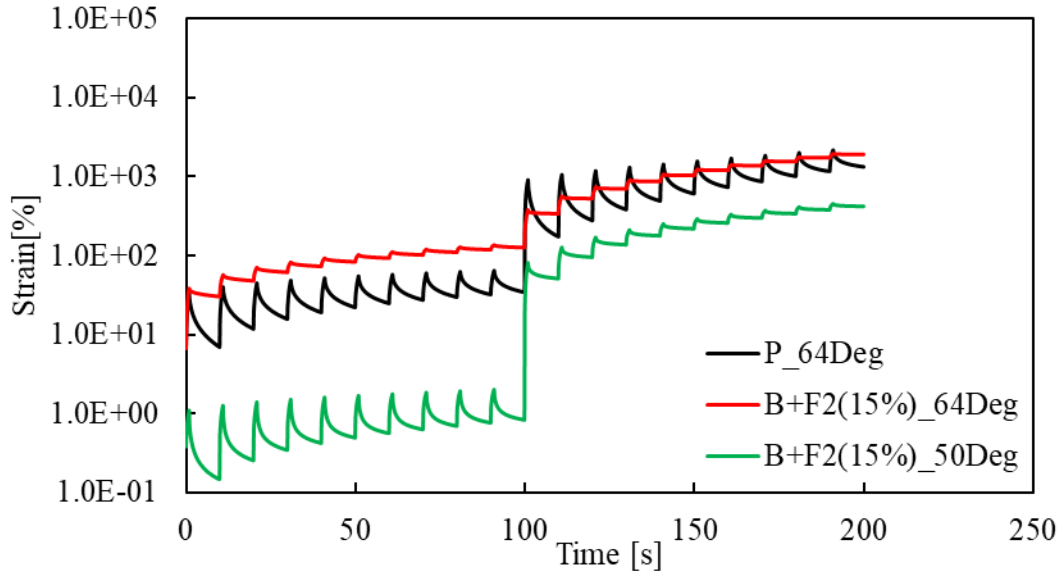
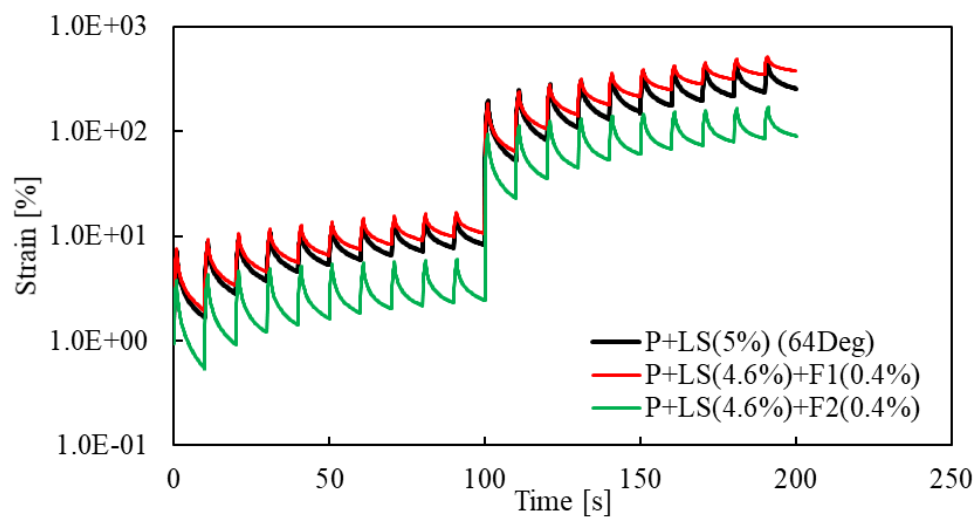
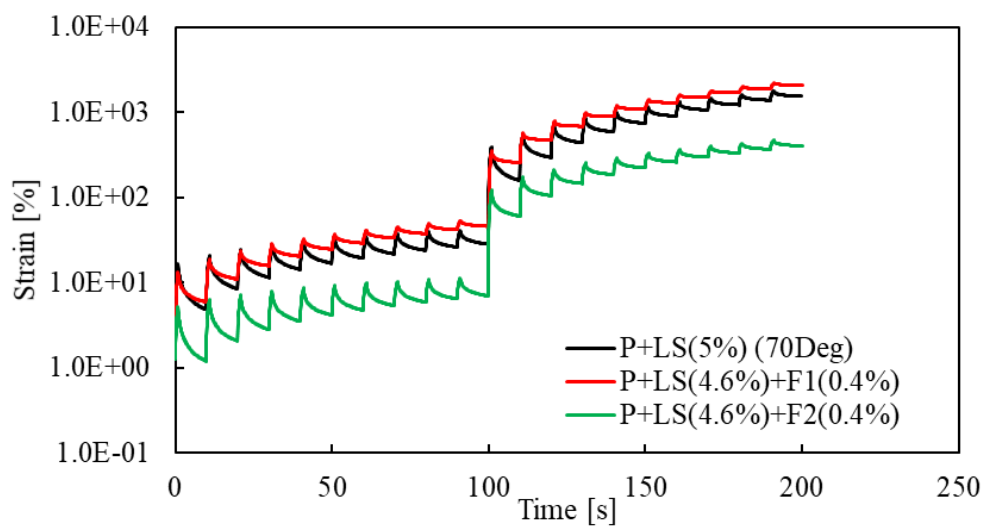


Figure 37: MSCR test result for P at 64 °C and B+F2(15%) case at 50 and 64 °C.

Similar investigation was carried out on mastic samples prepared by adding limestone filler to the PG 64-34 binder. In order to prepare the nano-modified samples, 0.4 percent of limestone filler was replaced by each of the two nano-fillers. The results of the MSCR tests on the mastic samples are shown in Figure 38. Test results showed an interesting trend. In the case of nano-filler F1, its effect on the resistance to permanent deformation was minimal or even negative compared to its reference case (P + LS), while nano-filler F2 improved rutting resistance throughout the temperatures ranging from 64 °C to 76 °C.



(a)



(b)

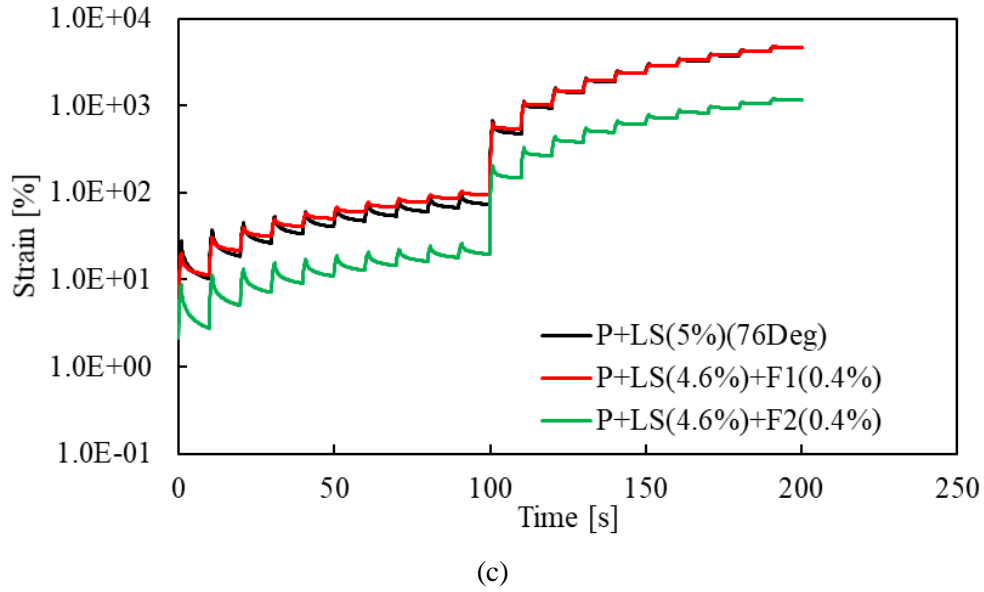
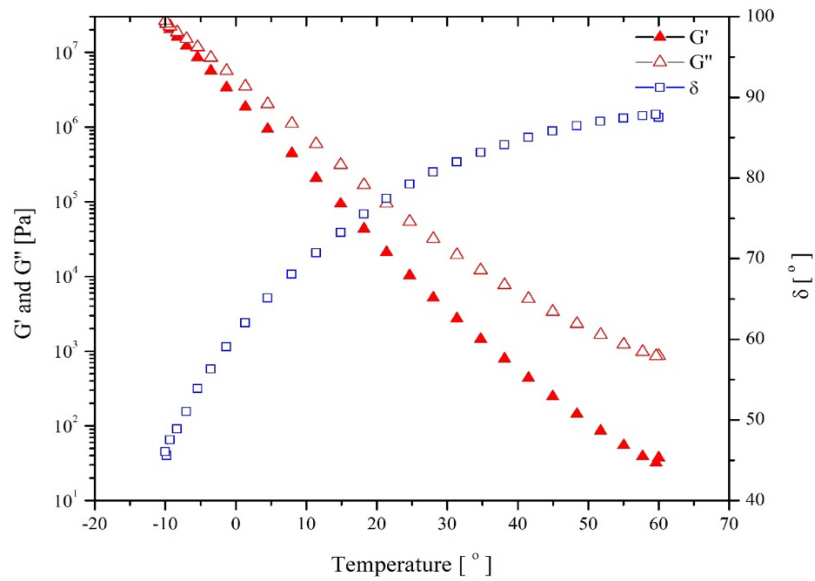


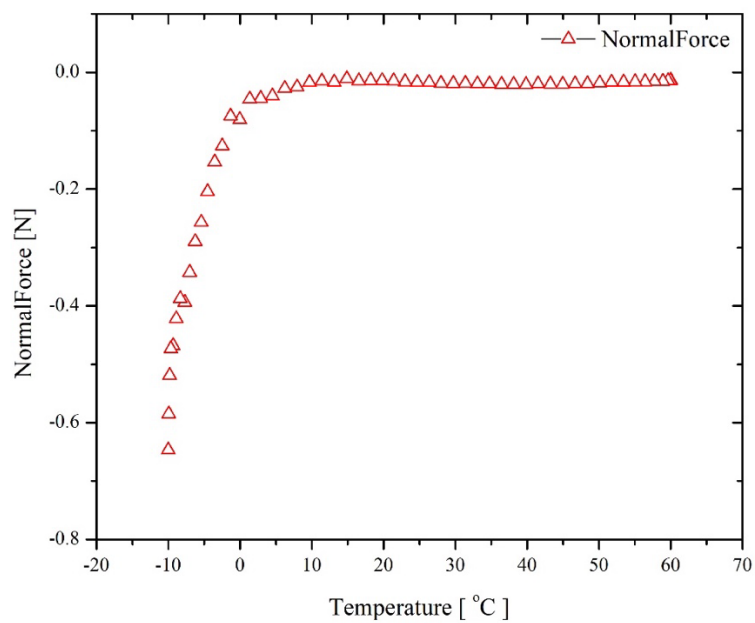
Figure 38: MSCR test results for base mastic and its nanomodified samples prepared by replacing part of the LS (a) 64°C, (b) 70°C, and (c) 76°C.

#### Temperature Sweep Test Results

Temperature sweep tests were also performed on each of the binder and mastic samples listed in Table 7 and Table 8. In these temperature-dependent sweep tests, individual samples were subjected to a linear temperature ramp from 60 °C to -10 °C at a rate of 5 °C /min and superimposed with an oscillatory loading. The loading was applied at a constant stress amplitude of either 0.5 kPa or 1.0 kPa at a constant frequency of 1.59 Hz. For the temperature sweep tests, the sample height and diameter was kept constant across all samples at 1-mm and 8-mm, respectively. Based on the preliminary testing-analysis, it was observed that when applying a constant strain amplitude loading, the instrument torque limit would be easily reached especially when the test temperature is below -5 °C due to high stresses within the samples. Hence, an oscillatory loading at a constant stress was utilized. Figure 39 shows the typical results for the temperature sweep test. As shown in the figure, the loss modulus ( $G''$ ) is higher than the storage modulus ( $G'$ ) which is confirmed by the phase angle results. As the temperature is lowered one can observe a temperature at which  $G'$  crosses over the  $G''$ . This transition temperature typically indicates the phase change of the material.



(a)



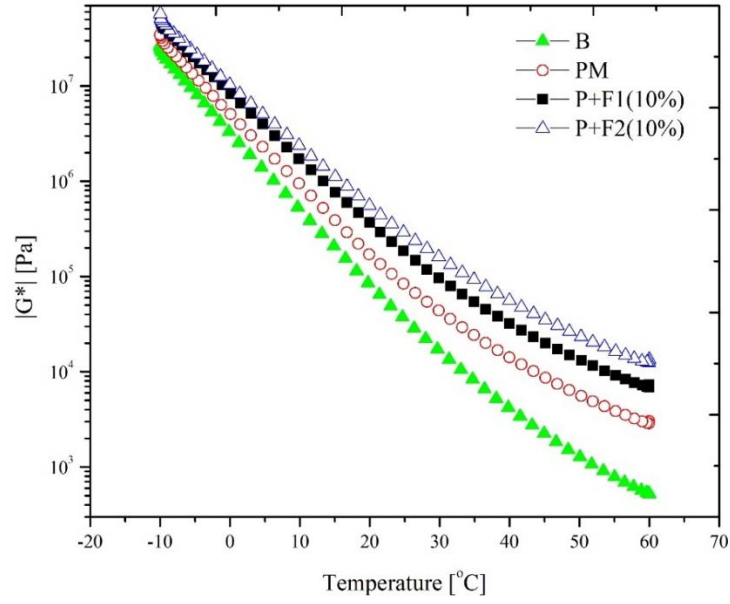
(b)

Figure 39: Temperature sweep results for binder showing (a)  $G'$ ,  $G''$ , and  $\delta$  vs temperature, and (b) normal force vs temperature.

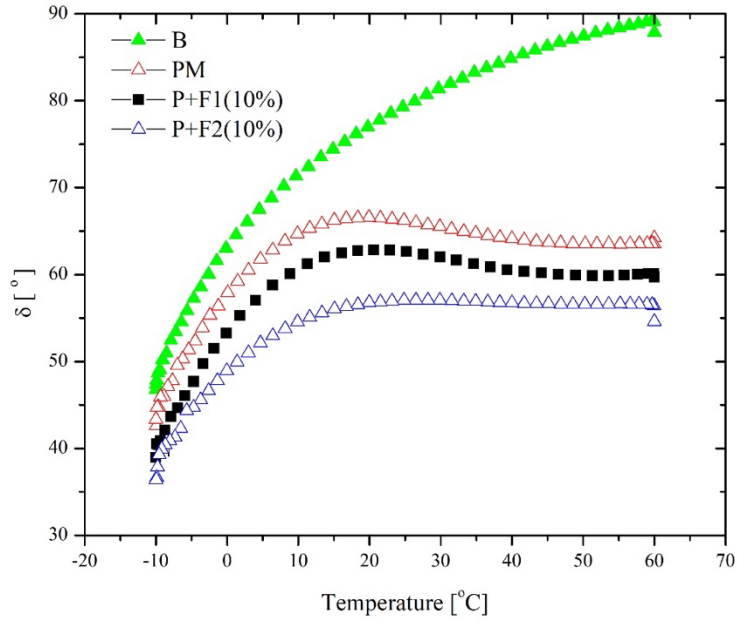
In Figure 40 and Figure 41, the temperature sweep results of the carbon nanofiller-modified binder and mastic are shown, respectively. In Figure 40, it can be observed that adding the graphite nanoparticles has increased the transition temperature regardless of the type of graphite filler added. This change may be attributed to the absorption of the lighter molecules by the graphite nanofillers causing increase of stiffness and transition temperature. Such interactions depend on the type of filler used as observed by different effects by the two fillers in Figure 40. Of the two graphite fillers, F2 influenced more the temperature susceptibility at low temperatures compared to F1. This can be observed in the shift of the transition temperature by 10 °C for the F2 modified binder compared to the base case.

Figure 41 shows the influence of carbon fillers in the presence of limestone filler. It shows that adding filler to the polymer modified (PM) binder increased the stiffness over the entire temperature range as shown in Figure 41(a). Also, addition of limestone filler caused a parallel shift of modulus values in the vertical direction indicating that the increase in stiffness is related to volumetric filling effects. This is further reinforced by the fact that the phase angle trends as a function of temperature are the same for binder PM and its limestone mastic as shown in Figure 41(b). It also shows that the temperature susceptibility of the PM binder and its limestone mastic (P+LS(5%)) is similar. Addition of filler F1 did not seem to change the properties whereas addition of filler F2 slightly increased the modulus and temperature susceptibility at low temperatures. One can conclude that, even though filler F2 showed improved performance in comparison to F1 at elevated temperatures, it is more susceptible to low temperature changes.



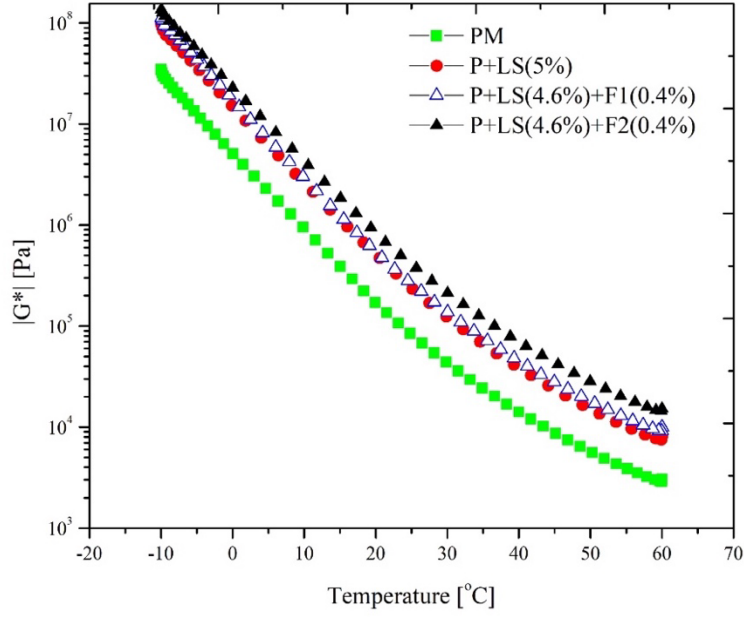


(a)

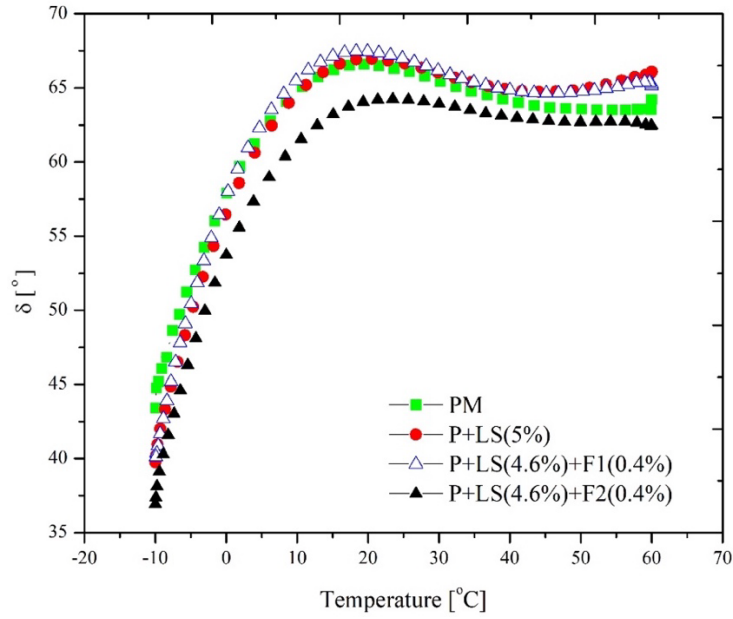


(b)

Figure 40: Temperature sweep results for base binder, polymer modified binder, and its nano-filler modified forms using filler F1 and F2: (a)  $|G^*|$  vs temperature, (b)  $\delta$  vs temperature.



(a)



(b)

Figure 41: Temperature sweep results for base polymer modified binder and its mastic forms modified with filler F1 and F2 (a)  $|G^*|$  vs Temperature (b)  $\delta$  vs Temperature.

## Chapter 5 Conclusions

This study investigated the feasibility of using natural fibers (i.e., cornhusk fibers) and nano-sized carbon-based modifiers to improve mechanical properties on asphaltic materials. Toward that end, the effect of natural cornhusk fibers on the resistance of two types of AC mixtures on cracking were tested for hot-mix asphalt (HMA) and cold-mix asphalt (CMA). In the second part of this study, two different types of carbon nano-fillers (F1 and F2) with different surface properties and sizes were added to two different asphalt binders: the base binder and the polymer modified binder. Also, mastic samples were prepared by replacing parts of the limestone filler by the carbon nano-fillers selected. Based on the test-analysis results, the following conclusions can be made.

- Cornhusk fibers proved to be tolerant to sustained high temperature (e.g., 160 °C) exposure associated with HMA preparation without significant degradation of mechanical property.
- The results showed slight improvements in cracking resistance in cornhusk reinforced HMA, and in the case of the CMA, Marshall flow. Overall, based on the test results, cornhusk reinforced HMA and CMA might not significantly improve critical mechanical properties given the added cost of fibers. In addition, cornhusk fibers proved difficult to properly disperse in HMA and CMA when mixed in laboratory. However, when fibers were mixed in an asphalt production plant, the fibers appeared to become more distributed.
- Nanoscale additives interacted with the binder quite differently. Additive F1 did not show a drastic improvement in the mechanical properties, fatigue resistance, and rutting resistance of the base and polymer modified binder at the mastic and the binder scale; however, additive F2 improved all the above-mentioned properties. From the experimental investigation, it is inferred that part of the polymer modification could be replaced by additive F2.
- Although additive F1 showed a minimal change, it could be useful in improving the secondary application of the pavement, such as the electrical conductivity, thermal conductivity, and absorption of radiation for energy storage, which was not the scope of this study but appears worthy to investigate as a future study. In addition, a pilot investigation that involves both fibers and nano-sized additives can further be considered.

## References

- AASHTO, T. (2009). "Standard method of test for multiple stress creep recovery (MSCR) test of asphalt binder using a dynamic shear rheometer (DSR)." American Association of State Highway and Transportation Officials, Washington, DC.
- Ahmad, F., et al. (2015). "A review: natural fiber composites selection in view of mechanical, light weight, and economic properties." Macromolecular Materials and Engineering **300**(1): 10-24.
- Aliha, M., et al. (2017). "The influence of natural and synthetic fibers on low temperature mixed mode I+ II fracture behavior of warm mix asphalt (WMA) materials." Engineering Fracture Mechanics **182**: 322-336.
- Ameri, M., et al. (2016). "Investigation of fatigue and fracture properties of asphalt mixtures modified with carbon nanotubes." Fatigue & fracture of engineering materials & structures **39**(7): 896-906.
- Andersen, S. I. and J. G. Speight (2001). "Petroleum resins: separation, character, and role in petroleum." Petroleum science and technology **19**(1-2): 1-34.
- Chatterjee, S., et al. (2005). Development of a Slump-Based Workability Test for Bituminous Maintenance Mixtures. Transport Research Board 85th Annual Meeting.
- Chen, H. and Q. Xu (2010). "Experimental study of fibers in stabilizing and reinforcing asphalt binder." Fuel **89**(7): 1616-1622.
- Chen, H., et al. (2009). "Evaluation and design of fiber-reinforced asphalt mixtures." Materials & Design **30**(7): 2595-2603.
- Dehghan, Z. and A. Modarres (2017). "Evaluating the fatigue properties of hot mix asphalt reinforced by recycled PET fibers using 4-point bending test." Construction and Building Materials **139**: 384-393.
- DoT, C. (2004). "Determination of Dust Proportion." from [http://www.dot.ca.gov/hq/esc/Translab/ormt/pdf/LP\\_4.pdf](http://www.dot.ca.gov/hq/esc/Translab/ormt/pdf/LP_4.pdf).
- Feng, Z., et al. (2012). "The relationship between colloidal chemistry and ageing properties of bitumen." Petroleum science and technology **30**(14): 1453-1460.
- FHWA (2015). "Public Road Length."

- Gallo, P. (2017). Asphalt mix reinforced with vegetable fibers. IOP Conference Series: Materials Science and Engineering, IOP Publishing.
- Ghile, D. B. (2006). "Effects of nanoclay modification on rheology of bitumen and on performance of asphalt mixtures." Delft, The Netherlands: Delft University of Technology.
- Golestani, B., et al. (2015). "Nanoclay application to asphalt concrete: Characterization of polymer and linear nanocomposite-modified asphalt binder and mixture." Construction and Building Materials **91**: 32-38.
- Im, S., et al. (2014). "Characterization of mode-I and mode-II fracture properties of fine aggregate matrix using a semicircular specimen geometry." Construction and Building Materials **52**: 413-421.
- Jahromi, S. G. and A. Khodaii (2009). "Effects of nanoclay on rheological properties of bitumen binder." Construction and Building Materials **23**(8): 2894-2904.
- Kaloush, K. E., et al. (2010). "Evaluation of fiber-reinforced asphalt mixtures using advanced material characterization tests." Journal of Testing and Evaluation **38**(4): 400-411.
- Khattak, M. J., et al. (2013). "Characterization of carbon nano-fiber modified hot mix asphalt mixtures." Construction and Building Materials **40**: 738-745.
- Khattak, M. J., et al. (2012). "The impact of carbon nano-fiber modification on asphalt binder rheology." Construction and Building Materials **30**: 257-264.
- Lee, S. J., et al. (2005). "Fatigue cracking resistance of fiber-reinforced asphalt concrete." Textile Research Journal **75**(2): 123-128.
- Liu, G., et al. (2011). "Influence of organo-montmorillonites on fatigue properties of bitumen and mortar." International Journal of Fatigue **33**(12): 1574-1582.
- Liu, X. and S. Wu (2011). "Study on the graphite and carbon fiber modified asphalt concrete." Construction and Building Materials **25**(4): 1807-1811.
- Lu, S.-N., et al. (2015). "Applications of nanostructured carbon materials in constructions: The state of the art." Journal of Nanomaterials **2015**: 6.
- MacAsphalt. "PRODUCT SHEET DATA." from <http://www.mcasphalt.com/sites/default/files/MCA%20PDS%20-%20Perma-Patch.pdf>.
- Mahrez, A., et al. (2005). "Fatigue and deformation properties of glass fiber reinforced bituminous mixes." Journal of the Eastern Asia Society for Transportation Studies **6**: 997-1007.

- Mansourian, A., et al. (2016). "Evaluation of fracture resistance of warm mix asphalt containing jute fibers." Construction and Building Materials **117**: 37-46.
- Michael J. Sprung, L. X. N., Matthew Chambers, Justyna Goworowska, Chris Rick and Joanne Sedor (2017). Freight Facts and Figures, FHWA.
- NCAT (2014) NCAT Researchers Explore Multiple Uses of Rejuvenators. **26**,
- NCAT (2014). NCAT Researchers Explore Multiple Uses of Rejuvenators, National Center for Asphalt Technology. **26**: 7-9.
- Nsengiyumva, G. (2015). "Development of Semi-Circular Bending (SCB) Fracture Test for Bituminous Mixtures."
- Ozer, H., et al. (2016). "Development of the fracture-based flexibility index for asphalt concrete cracking potential using modified semi-circle bending test parameters." Construction and Building Materials **115**: 390-401.
- Pan, P., et al. (2015). "Conductive asphalt concrete: A review on structure design, performance, and practical applications." Journal of Intelligent Material Systems and Structures **26**(7): 755-769.
- Pan, P., et al. (2014). "Influence of graphite on the thermal characteristics and anti-ageing properties of asphalt binder." Construction and Building Materials **68**: 220-226.
- Putman, B. J. and S. N. Amirkhanian (2004). "Utilization of waste fibers in stone matrix asphalt mixtures." Resources, conservation and recycling **42**(3): 265-274.
- QPRUSA (2014). "QPR Material Specifications." from [http://qprusa.com/wp-content/uploads/2014/02/QPR\\_Material\\_Specifications.pdf](http://qprusa.com/wp-content/uploads/2014/02/QPR_Material_Specifications.pdf).
- Reddy, N. and Y. Yang (2005). "Properties and potential applications of natural cellulose fibers from cornhusks." Green Chemistry **7**(4): 190-195.
- Reddy, N. and Y. Yang (2007). "Structure and properties of natural cellulose fibers obtained from sorghum leaves and stems." Journal of agricultural and food chemistry **55**(14): 5569-5574.
- Reddy, N. and Y. Yang (2009). "Properties and potential applications of natural cellulose fibers from the bark of cotton stalks." Bioresource technology **100**(14): 3563-3569.
- Rew, Y., et al. (2017). "Electrical and mechanical properties of asphaltic composites containing carbon based fillers." Construction and Building Materials **135**: 394-404.

- Santagata, E., et al. (2015). "Fatigue properties of bituminous binders reinforced with carbon nanotubes." International Journal of Pavement Engineering **16**(1): 80-90.
- Shanbara, H. K., et al. (2017). "Improving the Mechanical Properties of Cold Mix Asphalt Mixtures Reinforced by Natural and Synthetic Fibers." Airfield and Highway Pavements **2017**: 102.
- Subirana, M. and E. Y. Sheu (2013). Asphaltenes: fundamentals and applications, Springer Science & Business Media.
- Sun, Y., et al. (2017). "Self-healing performance of asphalt mixtures through heating fibers or aggregate." Construction and Building Materials **150**: 673-680.
- Tapkın, S. (2008). "The effect of polypropylene fibers on asphalt performance." Building and Environment **43**(6): 1065-1071.
- Watson, D., et al. (1998). "Georgia Department of Transportation's progress in open-graded friction course development." Transportation Research Record: Journal of the Transportation Research Board(1616): 30-33.
- Wu, S., et al. (2010). Preparation and fatigue property of nanoclay modified asphalt binder. Mechanic Automation and Control Engineering (MACE), 2010 International Conference on, IEEE.
- Xu, Q., et al. (2010). "Performance of fiber reinforced asphalt concrete under environmental temperature and water effects." Construction and Building Materials **24**(10): 2003-2010.
- Yao, H., et al. (2015). "Fourier Transform Infrared Spectroscopy characterization of aging-related properties of original and nano-modified asphalt binders." Construction and Building Materials **101**: 1078-1087.
- Yildirim, Y. (2007). "Polymer modified asphalt binders." Construction and Building Materials **21**(1): 66-72.
- You, Z., et al. (2011). "Nanoclay-modified asphalt materials: Preparation and characterization." Construction and Building Materials **25**(2): 1072-1078.